

PRECEDING PAGE BLANK NOT FILMED

N 72-29910

THE INFLUENCE OF MODIFICATIONS OF A FATIGUE LOADING HISTORY PROGRAM ON FATIGUE LIFETIME

By J. Branger
Eidgenössisches Flugzeugwerk
Emmen, Switzerland

SUMMARY

Rectangular specimens of 7075 and 2014 aluminum alloys with two holes (stress concentration factor of 3.24) have been tested under axial fatigue loading on a six-rod test bed with modifications of the loading program, the surface particulars, and the frequency. The length of the precrack stage was investigated by use of a new crack detector.

In most cases the two alloys behaved similarly, with similar life to crack start under the same loading. Some overloads lengthened the life. Truncation by omission of the lowest peak loads should be limited to about 20 percent of the ultimate load. Simplifying counting methods gave misleading results. Very thin surface layers of anodizing, protection by vinyl, dry nitrogen atmosphere, as well as stepwise reaming or grinding the surface of the holes, lengthened the life; thick anodized layers shortened the life. Compressing the hole surface by rolling had no influence. Frequencies at about 210 to 240 cpm produced shorter lives than those at 40 cpm. At 5.4 cpm the life was considerably longer. A model to better understand the precrack-stage fatigue mechanism is discussed.

15

INTRODUCTION

Fatigue test programs are usually designed to fit available test installations. Since the capability of most test facilities is limited, such test programs have to be simplified. The genuine sequence of the loading occurring in real flight usually has to be neglected. The influence of this neglect and also the influence of blocking cycles on the result of a fatigue test cannot be calculated by present methods nor can it be estimated because of many gaps in the knowledge of the fatigue mechanism. The need to remove these restrictions by appropriate tests is obvious. Test series considering the effect of variation of one or two parameters can help to find explanations of the fatigue mechanism or can at least prove whether proposed theories are possible or not.

Figure 1 represents a survey of the investigation of the influence of program modifications on the fatigue life of light alloy specimens. This paper is especially

dealing with the precrack stage of a specimen representing safe-life aircraft elements machined from bars and plates. Also, the crack-propagation life is considered to some extent.

Loading history which does not neglect the genuine sequence of the loads seems to be the only test approach to solve the problem. Moreover, since full loading history programs take a long time to run, means to shorten them without influencing the life to failure should be evaluated.

SYMBOLS

A	chemical affinity
a	index for arithmetical
b	index for probable, or for bending (σ_b)
C	crack-stage length, $C = F - P$
a_1, b_1, c_2, c_3	material, surroundings, and loading parameters
c'	quasi-cycle (asymmetric)
D	damage
D'	amount of damage produced by R' , that is, by the effective amount of reaction per cycle
D''	amount of damage produced by R'' , that is, by the reaction of one half-cycle
e	eccentricity
F	life to failure (number of cycles, flights or periods)
f	function
fi	flight number
fq	flight number per period

fs	scatter factor, $\frac{\bar{F}_{50}}{P_{99.9}}$
Hq	number of quasi-cycles of one period
I	intensity of incitation of chemical activity, $I = f(v) \cdot f(s)$
i	index for number of cycle, flight or period
$\left. \begin{matrix} K_1 \\ K_2 \end{matrix} \right\}$	stress concentration factors, calculated by RAS Data Sheets
L	load
Lq	highest peak load in one period
N	number (of cycles, flights or periods)
n	number of specimen; index for nominal
P	life to the end of the precrack stage, that is, to crack start (number of cycles, flights or periods)
p	duration of reaction = persistence (time)
q	period, index for period
R	reaction (chemical)
R'	effective amount of reaction per cycle
R''	amount of reaction in one half-cycle
S	strain, range of strain
s	empirical standard deviation $s = \left[\frac{1}{n-1} \sum_{i=1}^n (\log N_i - \log \bar{N})^2 \right]^{1/2}$
s_F	s for the number of periods up to failure

s_p	s for the number of periods up to the end of the precrack stage, that is, up to crack start
t	time
u	index for ultimate
v	rate of straining, dS/dt
y	probability of survival
z	electrical resistance
Δ	lowest considered load step
ν	rate of reaction (chemical), $f\left(I \cdot \frac{A}{\Omega}\right)$
σ	stress, load per unit of area
φ	function of
$\left. \begin{matrix} \psi_x \\ P \end{matrix} \right\}$	ordinate values for the third asymptotic extremal distribution (Smirnow)
Ω	chemical resistance
ω	frequency of cycles

A bar over a symbol denotes a mean value.

MEANS AND METHODS

The means and methods used by the Swiss Federal Aircraft Establishment (called F + W) for the investigation and evaluation of the influence of program modifications involve a six-rod test bed, a crack detector, test rods, fatigue loading history, and probable mean and scatter. For test specimens which are not too large, this problem can be investigated on the six-rod fatigue test bed (fig. 2), developed and built by F + W (ref. 1), because this facility is capable of simulating the genuine sequence of loads up to 8 tons for each specimen. A structural component of a shape commonly used in aircraft, already mentioned in reference 2, was chosen as the test specimen (fig. 3). It is a slightly eccentric, axially loaded, notched specimen of rectangular cross section. A

better insight into the behaviour of fatigue is due to the crack detector (figs. 4 and 5), also developed by F + W and operational since 1969 (ref. 3).

Figure 6 defines fatigue loading history, that is, a loading in which all actual service loads essential for fatigue are applied in their genuine sequence, magnitude, and frequency, and only rest times and steady loads are omitted. Figure 7 presents the symbols and also explains how the results of the tests are evaluated. Since six test specimens, each with two identical notches, are run simultaneously, each run is giving the scatter of 12 precrack stages and the scatter of the crack-propagation life of the faster growing crack in each specimen. As Freudenthal (ref. 4) explained, it is the time to the first failure which is important, especially for safe-life elements. Therefore, all the tests are evaluated in the manner presented in figure 7. The log-extremal paper was devised by Smirnow (ref. 5). Moreover, figure 7 defines the scatter factor.

The properties of the investigated 7075 and 2014 light alloys are presented in figure 8. The 2014 alloy plate was delivered in the prestretched (2 percent) condition. The test specimens machined from this plate were fully heat treated after they were machined.

The main data of the loading programs are listed in table I.

The investigation has four main considerations: influence of omission of low loads and addition of overloads (group A), influence of different counting methods (group B), influence of surface particulars (group C), and influence of frequency (group D). A survey of the test-run numbers is given in figure 9.

INVESTIGATIONS

Group A

The aim of group A (fig. 10) is to disclose the influence of omitting the lowest load steps, as well as the influence of adding some overloads (fig. 11). The history program applied is the VENOM Program (ref. 6) consisting of 350 flights; the full program is called VENOM Program II. By omitting the smallest air and ground loads, program XIV was deduced from program II. In similar manner, programs XV (only the smallest air loads omitted) and XVI (only the smallest ground loads omitted) were deduced from program II. On the proposal of Hooke of ARL in Melbourne, program XVII was deduced from program XIV by omitting the next smallest air and ground loads, whereas program XVIII was deduced from program II by addition of some high peak loads exceeding the design limit load. At each fifth period an overload of 107.5 percent and at the tenth period one of 115 percent were applied. All these programs strictly observe the genuine load sequence in all 350 flights.

Figure 12 presents the results of the investigations of group A. The data are listed in tables II and III.

Group B

There is still much speculation about the influence of different counting methods of the occurring fatigue loads on the fatigue life. Group B (fig. 13) is aiming to clear this. Although programs V' and VI' are deduced directly from program II by counting the peaks between the mean level crossings (these are the +1g level for V' and the zero-g level for VI'), LBF at Darmstadt composed two new programs: program XX by counting program II with the "level crossing" method and program XXI with the "range pair" method defined by Schijve (ref. 7), both furthermore pooling positive and negative peak loads and grouping the same cycles within each flight into blocks. This is represented on the right side of figure 13 by the hatching. The ground loads had to be presented separately.

More of the character of these program modifications is visible in figure 14. The differences from the basic program are evident.

Figure 15 and table IV present the results of group B, in which some comparative tests for specimens which were taken transversely from the plate were also included.

Group C

On the basis of a hypothesis proposed by Schaub (ref. 8) in 1955, the investigation project was completed by considering the influence of surface particulars. Figure 16 and table V give a survey of this test series and the results. Anodic surface treatments are very widely applied where cladding is not possible. Their influence on fatigue is not sufficiently known. It was decided to test surface-layer thicknesses of about 20μ and 6μ for anodic oxidation in sulfuric acid and 3 to 4μ for the anodic oxidation in chromic acid, known as the BF 4 procedure (a better defined version of Bengough). In most cases these treatments are applied before the holes are reamed; the same procedure was followed for these test specimens. It is of rather academic interest to hinder the chemical activity by a thin protective layer of vinyl as it is used to protect transistors or to lower the chemical affinity by an artificial atmosphere of commercially available dry nitrogen.

Similar to the tests of Schaub, test runs 69 and 71 were performed in such a manner that from time to time the holes 6.0 mm in diameter of the test rod were reamed or ground in steps of 0.1-mm diameter, up to five times, to a final diameter of 6.5 mm. Although by this procedure the net area was reduced by 2.5 percent and the stress concentration factor was increased from 3.24 to 3.30, the last crack started only at 115.2 periods on the reamed specimen and at 195.8 periods on the ground specimen (compared with 40.1 periods for the last crack start of those specimens which were reamed only once to a diameter of 6.0 mm). Therefore, to find the reason for the end of the precrack stage,

one needs to look only in the surface layer. This result confirms the findings of many authors. The very long life of the last three specimens after the last grinding is difficult to explain. Perhaps the workman did his job with extraordinary care because he knew what was expected and then produced a surface of higher quality than before.

No gain resulted from rolling the hole, notwithstanding the fact that it was made by a specialist.

Group D

The frequency effect on the fatigue life is still debated. It is therefore necessary to investigate its influence. Figure 17 and table VI present the results.

On a chain test bed 36 test rods of the same design were fatigue loaded parallel and simultaneously with the full-scale fatigue tests of three VENOM aircraft. The loading program I differs from program II only by those orders which were needed for the full-scale test; the loads, their sequence, and their number were exactly the same as with program II on the six-rod test bed. Both test beds are in the same room. The only differences were the frequency, 5.4 cpm (this test lasted $6\frac{1}{2}$ years!), and the shape of the cycles (fig. 18). As an intermediate frequency to 210 or 240 cpm, 40 cpm was selected because it can be run on the six-rod test bed and at the same strain rate as for 210 or 240 cpm.

For program II the increasing (56 and 340 percent) life with decreasing frequency from 240 cpm to 40 cpm and 5.4 cpm is remarkable. Another comparison test was run with program XX, once with 96 cpm and once with 173 cpm. The opposite behavior is noteworthy.

PRECRACK STAGE

Student's test was used to determine the significance of the difference indicated in the tables by the ratio of the precrack-stage lives \bar{P}_{50} . The probability levels for the differences considered are listed in table VII. Levels of about 90 percent or higher indicate a significant difference; lower ones may indicate a trend, whereas very low levels indicate that the modification had no influence on the life. In some cases the actual thickness of the anodized layer must be taken into account and in some cases also the fact that the specimens were manufactured from different bars (as indicated by the test number). Generally, table VII hints that the significance is higher for 2014 alloy. The reason is the higher loading relative to the ultimate load.

Influence of Alloy

The test specimens of 7075 alloy, as well as those of 2014 alloy, were loaded to exactly the same absolute load values. Relative to the ultimate strength, the 2014 speci-

mens were thus loaded about 33 percent higher than the 7075 specimens. Nevertheless, the fatigue life of 2014 is only 19 percent shorter than that of 7075 (table VIII). This result confirms the well-known fact that the fatigue strength of the different aluminum alloys is nearly independent of their static strength. By the way, a part of the difference may be contributed to the 7075 specimens being machined from bars 15 by 60 mm, whereas the 2014 specimens were cut in the longitudinal direction from plates 32 by 1220 by 2290 mm. This also explains the slightly higher scatter for 2014.

Influence of Overloads

As expected and as reported and explained by many authors for program loading, the overloads lengthened both stages (table II) but much more so with 2014. For this alloy the relative overload (relative to the ultimate strength) was much higher: The highest peak load applied (+6075 kp) is 53 percent of the nominal ultimate load for 7075 but 71 percent of that for 2014. Nevertheless, overloads should not be taken into account because not all service aircraft experience them.

Influence of Omitting Cycles With the Lowest Peak Loads

For 7075 anodized to 20μ the omission of the lowest and the next lowest peak loads (table III) has no significant influence on the life although the number of cycles is reduced by 81 percent. It seems that a favourable effect is abolished by another, unfavourable effect. In contrast, 2014 suffers a decrease in lifetime of 45 percent when the lowest peaks are truncated but has an increase of 63 percent when the next lowest peaks are also truncated. Relating programs XVII to XIV, this increase is as much as 195 percent. This increase of life may be explained by the truncation of the positive peaks at a relative level of 27.5 percent (relative to the ultimate load), whereas truncation at a level of 20.5 percent with 7075 has a slightly unfavourable effect. Taking into account the stress concentration factor of 3.24, the level of 27.5 percent is just at the nominal 0.2 yield strength of 2014, whereas the level of 20.5 percent is only at 77 percent of the nominal 0.2 yield strength of 7075. That is about the same for the lowest peak level omitted (program XIV) with 2014 (75 percent of 0.2 yield strength) where the effect is on the same side but faster. For these alloys, axial tension and compression, and a stress concentration factor of 3.24, the critical limit thus lies between 20.5 and 27.5 percent. Omitting loads smaller than this limit shortens the life, which seems to be very astonishing; whereas the omission of loads greater than this limit lengthens the life, as is expected. The strange shortening effect may be due to a recovery or a re-creation during the application of these lowest loads. This very interesting effect will be discussed further, in connection with surface influences and frequency.

Before the crack detector type 02 was developed, tests were performed with the same specimen and 7075 anodized to only 6μ . For the arithmetical mean of six specimens, the

ratio of program XIV to II was 0.89 at failure. Later tests on 2014 at a higher relative load level had a similar, more pronounced trend. The influence of omitting some of the ground load cycles will be discussed subsequently.

Influence of Counting Methods

The important decrease in the life by counting by the level-crossing method (program XX) has to be attributed mainly to the pooling of positive and negative peak loads into combined cycles. In the Swiss Review 1967 (ref. 1) a simplified test with the same 7075 specimen for the investigation of the pooling effect was reported. The pooled program (VIII) had a life ratio of 0.43 to that of the nonpooled program (XI), which is very near the ratios 0.34 for 7075 and 0.38 for 2014, when \bar{F}_{50} of program XX is compared with \bar{F}_{50} of program II.

The order-of-magnitude longer life with the program designed by the range-pair method (program XX) has to be attributed to the diminution of all positive peak loads, although such a big difference was not expected. It is noteworthy that both alloys behave nearly identically. Therefore, both counting methods have to be rejected. The same has to be said of the mean-crossing-peak counting method if this mean is zero (program VI') because this crude method omits too many cycles (fig. 14). The resulting increase of life was expected but perhaps not by this amount. About the same increase is valuable for the transversely machined 2014 specimens, as may be seen by comparing runs 100 and 97 in table IX. By putting the mean mainly at +1 of the air loads, only the ground loads are concerned. This will be discussed subsequently.

Influence of Surface Particulars

The unfavourable effect of a thick 20- μ anodized surface layer, which is hard and cracks easily, thus forming stress raisers, is well known. The decrease of only 30 per cent is even less than expected by many people. In contrast, the important favourable effect of a thin anodized layer was not expected, certainly not by this amount. It may be that these thin layers are so elastic that they do not crack and hence fulfill their protective task. The influence of the thickness of the anodized layers was more important than had been expected. Therefore, measurements of the layer thickness of all test specimens were made after the tests. These measurements disclosed considerable differences in the nominal thickness. By this way, a part of the scatter was better explained. The only procedure which regularly gives the same thickness with a high reliability seems to be the BF 4 process.

The smaller favourable effect of the vinyl protection may be due to low porosity, which also explains the greater scatter. The fact that the life in a nitrogen atmosphere was only doubled (other authors reported much higher ratios) may be explained by the test

conditions: Commercially available dry nitrogen was used, the specimen was not cooled down, and testing was at room temperature. But a very important fact has to be noted: By simple chemical means the crack stage, as well as the precrack stage, can be lengthened considerably although the mechanical fatigue strengthening of the specimen is strictly the same.

Removing about 0.05 mm of the surface layer, by reaming or grinding, confirms the work of Schaub and his collaborators. The removal was accomplished by the same manner in which the hole was machined at the beginning. To avoid the effect of a further factor, the specimens were not electropolished. Although the crack detector was working perfectly, the removal procedure was made too late in some cases. Nevertheless, the increase of the life of the last four ground specimens is extraordinary.

In contrast, the test with the surface compressive treatment by a rolling procedure was disappointing. The main reason may be that the crack always starts at the edge of the hole because the special shape of the test rod has a slight eccentricity. This reveals the doubtful effect of treatments like this – doubtful because eccentricities are not completely avoidable in actual designs.

Influence of Frequency

Up to now there have been only a few reports on tests with increasing life at decreasing frequency. A note from Schütz related Weller's (Dresden) work, who reports (ref. 9) on both trends and who advocated in 1966 (ref. 10) that there must exist a frequency-dependent minimum of life with increasing life in both directions, that is, by decreasing the frequency and by increasing it from that minimum. Weller's assumption is obviously right, as will be discussed later.

There are three factors contributing to the frequency-dependent effect:

1. The genuine corrosion of unstrengthened aluminum alloys (in the present test series this influence may be neglected).
2. The strain rate, which in most cases increases with increasing frequency. Test runs 67/68/73 and 64, 57, and 55 (table VI and fig. 18) eliminate this factor because the strain rate is the same in all cases.
3. The proper frequency effect. This one is of special interest and must be discussed in connection with other influences, for example, the influence of omitting cycles, counting methods, and surface particulars.

For test run A (program I, fig. 18) the strain rate was greatly reduced. This test reflects the influence of two factors, which may explain the very long life.

The opposite trend of test runs 57 and 55 is remarkable and may be attributed at first to the very different program and cycle shape. This difference seems to move the frequency of the minimum of life to about 100 cpm, whereas for the loading history program shape this minimum lies at about 200 to 250 cpm.

In 1956 Wade and Grootenhuis (ref. 11) found that the life still increases if the frequency is increasing from 24 Hz to 3835 Hz (1440 to 230 000 cpm). But Wood and Mason (ref. 12) reported in 1968 and 1969 that by increasing the frequency from 1700 cpm to the ultrasonic range of 17 000 Hz (1 million cpm), the life decreased considerably. Two new factors (resonance and concentration in a few localities) are responsible for this result.

Thus, after the minimum proposed by Weller, there is a maximum, detected by Wood and Mason, at about 5000 times higher frequencies, as presented in figure 19. This down-up-down configuration comes about by the effects of different factors which predominate in turn. This will be discussed by means of a model.

Influence of Compressive Loads

In these tests compressive loads are applied by ground loads and negative air loads. As the latter are very few compared with the ground loads, the findings reflect the importance of the ground loads.

Table X reveals opposite behaviour of 2014 and 7075 alloys. Program XVI, which omits all small ground load alterations (5 percent of ultimate load for 7075, 7 percent for 2014), gives shorter lives than program II in all three 7075 comparison tests (21 to 16, 76 to 67/68, and 104 to 92). This result is in accordance with the similar findings for program XIV for 7075. But in the 2014 comparison test the life with program XVI was longer than that with program II (test runs 88 to 91), which is not in accordance with the result of program XIV but with the result of program XVII. From this it may be deduced that the limit for ground loads, the omission of which has a life-lengthening effect, lies between 5 and 7 percent of the ultimate load, whereas the same limit for tension loads lies between 20 and 27 percent (as discussed in the section on omitting cycles). This result underscores the importance of compressive loads. The same trend of different behaviour appears in program V'.

Material Flow

Because of the integral design of modern wing skins, thick plates are needed which are machined as a whole. These plates are stretched to about 2 percent before machining. This procedure outweighs the effect of rolling the plates in respect to fatigue loading history, as can be seen in table IX. The time to failure is shorter only for the transverse-directed material with program V'. This result indicates a ground-load effect.

MODEL OF THE PRECRACK STAGE

In 1955 Schaub (ref. 13) put forward the following hypothesis: There must be two conditions for the start of a fatigue crack. One consists of the well-known physical-mechanical alterations due to fatigue loading; the other consists of a chemical reaction with the surrounding medium, which is derived from observations made by Kramer, Pepperhoff, and Churchill (ref. 13). On the same occasion it was mentioned that Gough and Sopwith, Weibull, Freudenthal, and others had found an important influence of the surrounding medium in classical constant-amplitude tests. Therefore, the inclusion of a chemical reaction for the explanation of the fatigue mechanism seems to be a more promising approach to clear the mystery of the precrack-stage fatigue mechanism than the physical-mechanical aspect alone. With the results of the tests on two aluminum alloys, this hypothesis may be refined by analysing a corresponding model of the first phase of fatigue damage, a scheme of which is presented in figure 20, and which may be called the "chemical phase."

1. Stress is inflicting strain (with all the well-known rules, especially important are those on the stress concentration factor and the residual stress originating from previous loadings (ref. 14)).

2. Strain, that is, the strain rate and the range of uninterrupted application of the variation of strain, is inciting chemical activity (apart from the well-known rules on the physical effects) between both mediums. By the way, steady strain is often the reason for stress corrosion, which should not be confused with the following description.

3. The intensity of incitation of this chemical activity, that is, the rate of reaction, is increasing with increasing strain rate and with increasing range.

4. This rate of reaction is more lively the better the affinity of these two mediums is and the lower the chemical resistance is.

5. The reaction may begin with a very short time delay after the inciting event but continues some time after it with decreasing intensity, like the persistence of a television screen.

6. The effect of this reaction is a new chemical product, most probably some composition between the two mediums concerned, that is, in most cases an oxide of the metal, in other words, damage.

7. The very thin layer of the genuine product of their affinity, for example 4 to 9 angstroms (10^{-10} m) of oxidation of aluminum alloys, does not hinder this activity if the inciting strain rate and range exceed a certain limit.

8. The (genuine) product produced at rest and the (artificial) product produced by strain rate and range are probably of the same nature, but the quantity of the latter is by far more rapidly increasing with continuing strain rate and range (called fatigue loading) than the former at rest.

9. Therefore, this accelerating (if not inciting at all) effect of the fatigue loading may be compared with the catalysis. Fatigue loading is, so to say, a dynamic catalyst.

10. This catalysis is producing an increasing thickness of the layer of the composition, for example, of the oxide, as long as fatigue loading continues.

11. There is no reason for a decomposition at rest.

12. The rate of increase in thickness will decrease with increasing thickness, as this effect begins to hinder the activity because of its chemical resistance. The rate of damage increase is thus decreasing. This is very important because a slowly increasing amount of damage explains the big scatter in the precrack stage of fatigue life, as will be seen later.

After this first phase of fatigue damage, a second phase, still in the precrack stage probably follows, which may be imagined as follows:

13. The layer of the new composition, for example this oxide layer has a Young's modulus different from that of the underlying metal, also a different yield strength. It is probably more brittle.

14. If the thickness of the layer exceeds a certain limit (which itself depends on the three-axial stress state), this layer may crack under a tension strain or form flakes under a compressive strain.

15. Those parts of the underlying metal, which are set free by these incidents and which get direct contact with the other medium, for example, with the atmosphere, will again be chemically activated, and so on.

16. Finally, the surface may get an aspect like the one which Wood (refs. 15 and 16) saw by scanning electron microscopy and on which a fatigue crack is starting.

The second part of the precrack stage may therefore be called the flake phase and is schematically presented by figure 21. Both these phases, that is, the whole process, is in fact a corrosion by fatigue and may be called fatigue corrosion, in contrast to corrosion fatigue, where a relatively quick genuine corrosion exists (and thus facilitates the fatigue corrosion). This definition differs somewhat from that given by McAdam (ref. 17), whose process "differs only in degree from stressless corrosion, but does not imply ordinary fatigue."

Most of these explaining steps are more or less evident. Step 2 was supposed by Schaub (ref. 8) 16 years ago and then supported by others. Step 15 was mentioned in 1960

by Broom and Nicholson (ref. 18). They also assumed a relation between fatigue deformation and hydrogen diffusion. Step 16 was detected only one and a half years ago by Wood (refs. 15 and 16) The increased oxide layer thickness (step 10) remains to be shown.

The most important supposition is step 5, the time-delaying activity, because by this persistence of a chemical process, the frequency influence may be explained as displayed in figure 20(g): By increasing the frequency, the reaction initially increases because of the not-yet-settled reaction of the preceding cycle; however, further increases in frequency decrease the relative damage per cycle. Obviously, together with step 3, the shape of the cycles (fig. 18) and their sequence are influencing the frequency at which the minimum life (fig. 19) is found; thus the seemingly opposite behaviour of programs II and XX is explained. Similar to figure 20(g) the omission of less effective, very low peaks (step 3) increases the value of the effective amount of reaction per cycle (and thus shortens the precrack life), whereas the crack-stage length increases by this same omission as expected (in table III compare test runs 74 with 73 and 86 with 91), thus supporting the hypothesis that the reason that the omission of the lowest peaks has a life-shortening effect originates entirely in the first damage phase.

Step 7 may explain the endurance limit to some extent. Finally, the larger scatter of the precrack stage may be explained by figure 20(h), as outlined in step 12.

The ultrasonic frequency range is not mentioned in this model because other factors are predominant and because frequencies higher than about 300 cpm do not occur in primary aircraft structures. But the model should still be valuable for acoustic fatigue (most at about 200 000 cpm).

CRACK-PROPAGATION STAGE

Because the crack-propagation stage is not the topic of this paper, only some unusual observations are mentioned.

1. The type F + W crack detectors can detect the crack depth as well as the fatigue crack surface before final failure. Figure 22 presents a fatigue failure surface and the corresponding record from the detector. The record is not a linear, but an exponential, function. Its character also depends on the shape of the specimen.

2. The crack stage is short, much shorter than often reported or assumed, when differentiated from the precrack stage.

3. The crack stage is, on the whole, of an astonishingly constant length (fig. 23), which was computed as outlined in the appendix by P. Gschwind.

4. Crack-stage lives decrease with decreasing probability of survival (i.e., longer life), for example, by some hardening effect. (See test runs presented in fig. 23(a).) A

low frequency combined with a small strain rate showed a remarkably large effect (run A, fig. 18). Nitrogen atmosphere (72), high overloads (90), and low frequency (64) also had an effect.

5. Crack-stage lives increase with increasing precrack-stage lives, for example, by some weakening effect. (See test runs in fig. 23(c).) This result was most pronounced for run 100 (transverse, most simplified program).

6. Very short crack-stage lives were experienced with program XX.

7. The computation of the relative crack-stage life, that is, $\frac{\bar{C}_{50}}{\bar{F}_{50}} \cdot 100$, reveals astonishingly high and consistent values of 10 to 30 percent.

8. As was shown in Stockholm (ref. 19), the fatigue-cracked surface, as recorded by the crack detectors, is increasing by a simple law and with a very low scatter, which can be seen in figure 24.

CUMULATIVE DAMAGE

The different character of the damage cumulation of the three phases of the model is presented in figure 25. The poor correlation of actual life until crack start with simple linear cumulative damage hypothesis originates mainly from the first phase, which reveals the influence of load sequence, cycle shape, and frequency. The proposed model is still a simplification and needs many tests to find quantitative coefficients, but it is hoped that the model helps for a better approach to the problem.

CONCLUSIONS

Up to now results from the test project permit the following conclusions:

1. There is no important difference in time to crack start between these two alloys (2014 and 7075) if loaded to identical values. This result confirms earlier findings.

2. Overloads have a favourable effect. This result is also in agreement with findings of earlier and less sophisticated tests. This should, nevertheless, not be considered for calculations of time to failure.

3. Omission of low peaks does not affect the time to failure of tests if this omission concerns peaks lower than about 20 percent of the ultimate load at tension and 5 percent at compression.

4. Counting load occurrences by the so-called peak between +1g mean-crossing method, peak between zero-g mean-crossing method, level-crossing and range-pair

methods (both combined with pooling and blocking) is giving misleading results and must be rejected.

5. While thick ($\sim 20 \mu$) sulfuric anodized surface layers have an unfavourable effect on the lifetime, the contrary is true for thin ($\sim 6 \mu$) layers or BF 4 treated elements, which lengthen the life.

6. Stepwise reaming or grinding of holes can lengthen the life considerably, which may be useful for maintenance people; whereas rolling of hole surfaces alone has no effect.

7. There is a definite frequency effect with a minimum and a maximum.

8. There is a strain-rate effect – decreasing rate giving increasing life.

9. A model, assuming a catalytic effect of fatigue loading on the chemical activity of the surface, with a persistence of this activity, is presented, which could explain the influences of frequency, strain rate, and load sequence, as well as the trend of decreasing life by omission of the lowest (and most numerous) peaks. The model also reveals an important reason for the scatter in the precrack stage.

10. The crack stage, now easier to observe by a new crack detector, is (for machined specimens) short – much shorter than often reported. It is, on the whole, of an astonishingly constant length, with a lower scatter than the precrack stage, which also diminishes the scatter of the life to final fatigue failure.

ACKNOWLEDGMENTS

Many thanks are extended to the collaborators for their help: Mr. P. Gschwind for the mathematical part, Mr. E. Eberle for evaluation and figures, Miss L. Meierhans for typewriting, Mr. L. Richiger for tables, and Mr. K. Steiner and his team for the editing of this report, also many thanks to Mr. E. Kindlimann (hydraulics) and Mr. H. Widmer (electronics) and their teams for keeping the test beds and recorders running day and night.

This paper is published with the permission of G.R.D. (Armament, Technology and Procurement Group of E.M.D.), Berne, Switzerland.

APPENDIX

COMPUTATION OF THE MEAN CRACK-STAGE LIFE

By P. Gschwind

Let $P(y)$ be the most probable line of precrack-stage life on log-extremal paper and $F(y)$ be the most probable line of fatigue failure, both functions of life expectancy y . The mean crack-stage life must be computed,

$$C(y) = F(y) - P(y) \tag{1}$$

On log-extremal paper (u, Y) a straight line is defined by two constants

$$Y = a_2 u + a_1$$

and

$$u = \frac{1}{a_2} (Y - a_1)$$

For F and P , then

$$u_F = \frac{1}{a_2^F} (Y - a_1^F)$$

and

$$u_P = \frac{1}{a_2^P} (Y - a_1^P)$$

Because u is the common logarithm of F and P ,

$$\left. \begin{aligned} F &= 10^{\frac{1}{a_2^F} (Y - a_1^F)} \\ P &= 10^{\frac{1}{a_2^P} (Y - a_1^P)} \end{aligned} \right\} \tag{2}$$

APPENDIX – Concluded

Otherwise on log-extremal paper,

$$y = e^{-e^Y}$$

or

$$Y = \log(-\log y) \tag{3}$$

Introducing equation (3) into equations (2) and (1) yields

$$C(y) = 10^{\frac{1}{a_2^F} \left[\log(-\log y) - a_1^F \right]} - 10^{\frac{1}{a_2^P} \left[\log(-\log y) - a_1^P \right]}$$

The constants a_1^F , a_2^F , a_1^P , and a_2^P are to be calculated with the least-square method from experimental data.

REFERENCES

1. Branger, J.: Swiss Review 1965 – 1967. ICAF Doc. 412, Minutes of the Tenth ICAF Conference, J. Y. Mann, ed., 1967.
2. Branger, J.: Swiss Review 1961 – 1963. ICAF Doc. 271, Minutes of the Eighth ICAF Conference, V. Villa, ed., 1963.
3. Branger, J.: Life Estimation and Predicting of Fighter Aircraft. Proc. Int. Conf. on Structural Safety and Reliability, A. M. Freudenthal, ed., 1969.
4. Freudenthal, A. M.: Reliability Analysis Based on Time to the First Failure. Proc. of Fifth ICAF Symposium, J. Y. Mann and I. S. Milligan, eds., Pergamon, 1967.
5. Smirnow, N. W.; et al.: Mathematische Statistik in der Technik. VEB Deutscher Verlag der Wissenschaften, 1963.
6. Branger, J.: The VENOM Program, F + W S-197 (not yet published).
7. Schijve, J.: The Analysis of Random Load-Time Histories With Relation to Fatigue Tests and Life Calculations. Fatigue of Aircraft Structures, W. Barrois and E. L. Ripley, eds., Macmillan Co., 1963, pp. 115-149.
8. Schaub, C.; and Liedtke, W.: Der Mechanismus des Dauerbruchs metallischer Werkstoffe. Colloquium on Fatigue, W. Weibull and F. K. G. Odquist, eds., Springer, 1956.
9. Weller, J.: Die Bedeutung der Lastspielfrequenz beim Dauerschwingversuch metallischer Proben a.s.o. in Neue Hütte, 6. Jg., Dez. 1961.
10. Weller, J.: Kritischer Vergleich einer Auswahl von Aluminium-Konstruktionswerkstoffen a.s.o. in IfL-Mitt. 5, Heft 12, 1966.
11. Wade, A. R.; and Grootenhuis, P.: Very High-Speed Fatigue Testing. International Conference on Fatigue of Metals, I. Mech. Eng., 1956.
12. Wood, W. A.; and Mason, W. P.: Fatigue Mechanism in Iron at Ultrasonic Frequency. J. Appl. Phys., Oct. 1969.
13. Lissner, O.: Einige Versuche über die Vorgänge in der Oberflächenschicht von Ermüdungsproben. Colloquium on Fatigue, W. Weibull and F. K. G. Odquist, eds., Springer, 1956.
14. Haibach, E.; Schütz, D.; and Svenson, O.: Forschungsbericht FB 78/68 des LBF. ICAF Doc. 508, 1969.
15. Wood, W. A.: Fatigue Crack Initiation as Viewed by Scanning Electron Microscopy. Technical Report No. 1, George Washington Univ., Jan. 1970.

16. Wood, W. A.: Elastic Fatigue in Titanium Studied by Scanning Electron Microscopy. Technical Report No. 2, George Washington Univ., Apr. 1970.
17. McAdam, D. J.: The Influence of Stress Range and Cycle Frequency on Corrosion. Proc. ASTM 30 (1930), Part 2, pp. 411-447.
18. Broom, T.; and Nicholson, A.: Atmospheric Corrosion-Fatigue of Age-Hardened Aluminium Alloys. Journal of the Institute of Metals, vol. 89, 1960.
19. Branger, J.; and Ronay, M.: High Strength Steels Under Fatigue History Loading. ICAF Doc. No. 499, Proc. of the Technical Session of the 11th ICAF Meeting, G. Wallgren and S. Eggwertz, eds., 1969.

TABLE I.- DATA OF LOADING PROGRAMS

Program	Cycles H_q in one period q of 350 flights			Highest peak loads L_q in one period q , kp	
	Air	Ground	Total	Positive	Negative
	II	20033	18515	38548	5265
V'	19553	350	19903	5265	-1600
VI'	638	350	988	5265	-1600
XIV	9180	3405	12585	5265	-1600
XV	9180	18515	27695	5265	-1600
XVI	20033	3405	23438	5265	-1600
XVII	6499	835	7334	5265	-1600
XVIII	20033	18515	38548	6075	-1600
XX			10150	5010	-1580
XXI			10150	4800	-1580

These data are valuable for both alloys investigated, also for all surface particulars and for all frequencies. All tests were run with the test rod (fig. 4) and all in the same test room at a room temperature of 15° to 20° C.

TABLE II.- OVERLOAD

Test run	Alloy 7075; 240 cpm							Alloy 2014; no anodic treatment; 210 cpm						
	s_F	s_P	\bar{c}_{50}	\bar{F}_{50}	\bar{P}_{50}	Anodic treat., μ	Program	\bar{P}_{50}	\bar{F}_{50}	\bar{c}_{50}	s_P	s_F	Test run	
77	0.0699	0.0939	6.3	37.1	30.8	16.5	XVIII	41.6	53.1	11.5	0.1015	0.0673	90	
73	.0408	.0550	4.9	32.8	27.9	20.3	II	30.4	38.3	7.9	.0774	.0576	91	
	1.71	1.71	1.28	1.13	1.10		XVIII II	1.37	1.38	1.46	1.31	1.17		

TABLE III.- TRUNCATION

Test run	Alloy 7075; 240 cpm						Program	Alloy 2014; no anodic treatment; 210 cpm					
	S _F	S _P	C ₅₀	F ₅₀	P ₅₀	Anodic treat., μ		P ₅₀	F ₅₀	C ₅₀	S _P	S _F	Test run
67/68	0.0630	0.0882	6.7	32.9	26.2	23.7	II	30.4	38.3	7.9	0.0774	0.0576	91
73	.0408	.0939	4.9	32.8	27.9	20.3	II	16.8	25.9	9.1	.1448	.1107	86
74	.0999	.1249	8.2	34.3	26.1	20.5	XIV	23.8	35.1	11.4	.0753	.0900	87
75	.1103	.1362	9.3	32.2	22.9	19.7	XV	49.7	61.8	12.1	.0823	.0606	89
79	.0628	.1020	7.0	31.3	24.3	24	XVII	0.55	0.68	1.15	1.87	1.92	
	2.45	1.33	1.67	1.05	0.94		Ratios: 74/73	1.63	1.61	1.53	1.06	1.05	
	1.00	1.16	1.04	.95	.93		79/ 67/68	2.95	2.38	1.33	.57	.55	
	.63	.82	.85	.91	.93		79/74	.78	.92	1.45	.97	1.56	
	2.70	1.45	1.90	.98	.82		75/73	1.42	1.35	1.25	.52	.81	
	1.10	1.09	1.13	.94	.88		75/74						
16	0.0452		F _a =	86.2		5.2	II						
20	.0602			76.8		7.7	XIV						
19	.1064			97.3		7.9	XV						
	1.77			1.27			Ratios: 19/20						
	1.33			.89			20/16						

TABLE IV.- COUNTING METHODS

Alloy 7075										Alloy 2014; no anodic treatment; 210 cpm				
Test run	s _F	s _P	\bar{c}_{50}	\bar{F}_{50}	\bar{p}_{50}	Freq., cpm	Anodic treat., μ	Program	\bar{p}_{50}	\bar{F}_{50}	\bar{c}_{50}	s _P	s _F	Test run
67/68	0.0630	0.0882	6.7	32.9	26.2	240	23.7	II	30.4	38.3	7.9	0.0774	0.0576	91
96	.0629	.0880	6.8	35.9	29.1	210	22.8	V'	54.4	64.7	10.3	.1347	.1265	101
	1.00	1.00	1.02	1.09	1.11			V'/II	1.79	1.69	1.30	1.74	2.20	
92	0.0825	0.0688	13.8	81.9	68.1	210	5.5	II						
102	.0561	.0716	19.2	122.0	102.8	210	3.3	VI'	74.8	93.4	18.6	0.1208	0.1078	99
103	.0952	.0965	12.3	83.0	70.7	210	5	V'						
	0.68	1.04	1.39	1.49	1.51			VI'/II	2.46	2.44	2.35	1.56	1.87	
	.59	.74	1.56	1.47	1.45			VI'/V'	1.37	1.44	1.81	.90	.85	
Alloy 7075										Alloy 2014; no anodic treatment; 96 cpm				
54/56	0.0478	0.0547	7.9	46.5	38.7	240	21.6	II						
55	.0445	.0893	3.5	15.8	12.3	96	21.2	XX	10.2	14.5	4.3	0.1102	0.1034	93
84	.0709	.0813	12.0	121.0	109.0	96	25.5	XXI	25.5	143.0	17.5	.1490	.1303	94
	0.93	1.63	0.44	0.34	0.32			XX/II	0.34	0.38	0.54	1.42	1.80	
	1.46	1.12	2.18	3.70	4.0			XXI/II	4.15	3.73	2.19	1.93	2.26	
	1.57	.69	5.0	10.9	12.5			XXI/XX	12.2	9.8	4.1	1.36	1.26	

TABLE V.- SURFACE

Alloy 7075; program II; 210 to 240 cpm					Alloy 2014; program II; 210 cpm							
Test run	s _F	s _P	c ₅₀	F ₅₀	P ₅₀	Surface particulars	P ₅₀	F ₅₀	c ₅₀	s _P	s _F	Test run
67/68	0.0478	0.0737	8.0	45.6	37.6	No treatment ①	30.4	38.3	7.9	0.0774	0.0576	91
						Std. atm.						
73	0.0408	0.0939	4.9	32.8	27.9	②a 20.3μ						
67/68	.0630	.0882	6.7	32.9	26.2	②b 23.7μ						
92	0.0825	0.0688	13.8	81.9	68.1	③ Anodic 5.5μ BF4 3.0μ	35.3	44.7	9.4	0.1513	0.1201	98
70	0.0779	0.1023	10.6	64.1	53.4	④ Viny ¹						106
72	0.0516	0.0716	15.3	92.7	77.4	No treatment ⑤ Nitrogen						105
						Ratios:						
	0.85	1.27	0.61	0.72	0.74	②a / ①						
	1.32	1.20	.84	.72	.70	②b / ①						
	1.73	.94	1.73	1.80	1.81	③ / ①	1.16	1.17	1.19	1.95	2.08	
	1.63	1.39	1.33	1.41	1.42	④ / ①						
	1.08	.97	1.91	2.03	2.06	⑤ / ①						
						No anodic ⑥						
80	0.0760	0.0641	7.5	44.5	37.0	Rolled surface						
	1.59	0.87	0.94	0.96	0.98	⑥ / ①						

TABLE VI.- FREQUENCY

Test run	Alloy 7075							Alloy 2014; no anodic treatment					
	Anodic treat., μ	s_F	s_P	\bar{C}_{50}	\bar{F}_{50}	\bar{P}_{50}	Program Frequency, cpm	\bar{P}_{50}	\bar{F}_{50}	\bar{C}_{50}	s_P	s_F	Test run
67/68/73	22.0	0.0487	0.0728	5.5	32.7	27.2	II II	30.4	38.3	7.9	0.0774	0.0576	91
64	21.2	0.0484	0.0724	8.0	50.5	42.4	II 40 40						107 (3 rods)
A	19.7	0.0286	0.0630	30.0	150.0	120.0	I 5.4 40						Nitrogen atm (107.3 r)
		1.00	1.00	1.46	1.55	1.56	40/ 240 210						
		.59	.86	5.5	4.6	4.4	5.4/ 240 40						
							Program XX Freq., cpm						
57	21.7	0.0693	0.0671	3.7	18.2	14.5	173						
55	21.2	.0445	.0893	3.5	15.8	12.3	96						
		0.64	1.33	0.95	0.87	0.85	96/ 173						

TABLE VII.- STUDENT'S SIGNIFICANCE TEST

- ① Test run considered
 ② Test run compared with
 ③ Probability level for the difference
- Actual thickness of anodized layer in μ
- ◆ Analogous relation for 2014 and 7075 alloy and same trend
 ✱ Analogous relation for 2014 and 7075 and opposite trend

①		②		③ %	①		②		③ %
No.	μ	No.	μ		No.	μ	No.	μ	
67/68	no	91	no	89	67/68	no	67/68	23.7	99
86	no	91	no	99	◆ 74	20.5	73	20.3	26
87	no	91	no	99	◆ 75	19.7	73	20.3	92
88	no	91	no	98	✱ 76	22.5	67/68	23.7	60
					◆ 104	7.5	92	5.5	>99
89	no	91	no	99	✱ 79	24.0	67/68	23.7	75
90	no	91	no	99	◆ 77	16.5	73	20.3	51
93	no	91	no	➤99	◆ 55	21.2	54/56	21.6	➤99
94	no	91	no	➤99	◆ 84	25.5	67/68	23.7	➤99
97	no	91	no	96					
98	BF4	91	no	85	◆ 67/68	no	92	5.5	99
99	no	91	no	99	◆ 102	3.3	92	5.5	>99
100	no	97	no	>99	◆				
101	no	91	no	>99	◆ 103	5.0	92	5.5	40
					◆ 96	22.8	67/68	23.7	49
105	N2	91	no		◆ 72	N2	67/68	no	99
106	Vinyl	91	no		◆ 70	Vinyl	67/68	no	97
107	no	91	no		◆ 64	21.2	73	20.3	99
95	no	101	no	>99	◆ 55	21.2	57	21.7	65
100	no	99	no	20	◆ 80	roll.	67/68	no	10
99	no	101	no	92	◆ 102	3.3	103	5.0	>99
100	no	95	no	>99	◆				
87	no	86	no	98	✱ 75	19.7	74	20.5	85
89	no	86	no	➤99	✱ 79	24.0	74	20.5	90.5

TABLE VIII.- ALLOY

Test run	Alloy	Surface treatment	Program	Frequency, cpm	\bar{p}_{50}	\bar{F}_{50}	\bar{C}_{50}	s_p	s_F
67/ 68	7075	None	II	240	37.6	45.6	8.0	0.0737	0.0478
91	2014	None	II	210	30.4	38.3	7.9	.0774	.0576
Ratio $\frac{2014}{7075}$					0.81	0.84	0.99	1.05	1.20

TABLE IX. - MATERIAL FLOW

Test run	Alloy	Flow direction	Program	Surface treatment	Frequency, cpm	\bar{P}_{50}	\bar{F}_{50}	\bar{C}_{50}	s_p	s_F
91	2014	Long.	II	None	210	30.4	38.3	7.9	0.0774	0.0576
97	2014	Trans.	II	None	210	36.7	42.5	5.8	.0705	.0514
Transverse/Longitudinal										
						1.20	1.11	0.73	0.91	0.89
101	2014	Long.	V'	None	210	54.4	64.7	10.3	1.347	0.1265
95	2014	Trans.	V'	None	210	35.0	38.1	3.1	.1473	.1283
Transverse/Longitudinal										
						0.64	0.59	0.30	1.09	1.01
99	2014	Long.	VI'	None	210	74.8	93.4	18.6	0.1208	0.1078
100	2014	Trans.	VI'	None	210	72.1	87.4	15.3	.0729	.0869
Transverse/Longitudinal										
						0.96	0.94	0.82	0.60	0.81
Ratio 100/97										
						1.97	2.06	2.64	1.03	1.69
100/95										
						2.06	2.30	4.94	.50	.68

TABLE X.- GROUND LOADS

Test run	Anodic treat., μ	Alloy 7075						Program	Alloy 2014; no anodic treatment					
		s_F	s_P	\bar{C}_{50}	\bar{F}_{50}	\bar{P}_{50}			\bar{P}_{50}	\bar{F}_{50}	\bar{C}_{50}	s_P	s_F	Test run
67/68	23.7	0.0630	0.0882	6.7	32.9	26.2	II	30.4	38.3	7.9	0.0774	0.0576	91	
76	22.5	.0407	.0729	6.2	27.0	20.7	XVI	43.6	52.2	8.6	.1367	.1085	88	
96	22.8	.0629	.0880	6.8	35.9	29.1	V'	54.4	64.7	10.3	.1347	.1265	101	
		0.79	0.83	0.93	0.82	0.79	XVI/II	1.43	1.36	1.09	1.77	1.88		
		1.00	1.01	1.02	1.09	1.11	V'/II	1.79	1.69	1.30	1.74	2.20		
		Alloy 7075							7075:	F_a		s_F	Anodic treat., μ	Test run
92	5.5	0.0825	0.0688	13.8	81.9	68.1	II		86.2			0.0452	5.2	16
104	7.5	.0902	.114	8.0	56.6	48.6	XVI		66.5			.0780	5.3	21
103	5.0	.0952	.0965	12.3	83.0	70.7	V'							
		1.09	1.62	0.58	0.69	0.71	XVI/II		0.77					
		1.15	1.40	.89	1.01	1.04	V'/II					1.73		

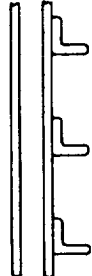


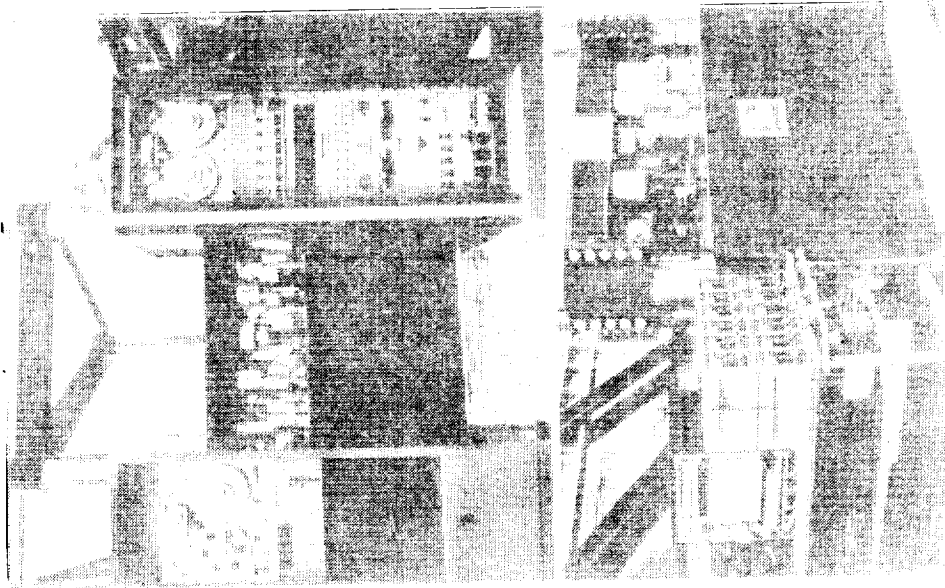
<p style="text-align: center;">Survey of the Investigation of the Influence of Program Modifications on the Fatigue Life of Light Alloy Specimens</p>				
Light Alloy Element or Component	Sheet 	Rod, Boom 	Plate 	
Crack Propagation	slow	fast	very fast	
Fatigue Behaviour	Fail safe	safe Life	safe Life	
Pre-crack Stage		Field of this Report		
Crack Propagation Life				
Life to Failure				

Figure 1



Six-Rod Fatigue Test Bed (F+W)

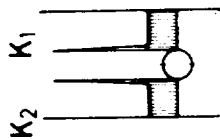
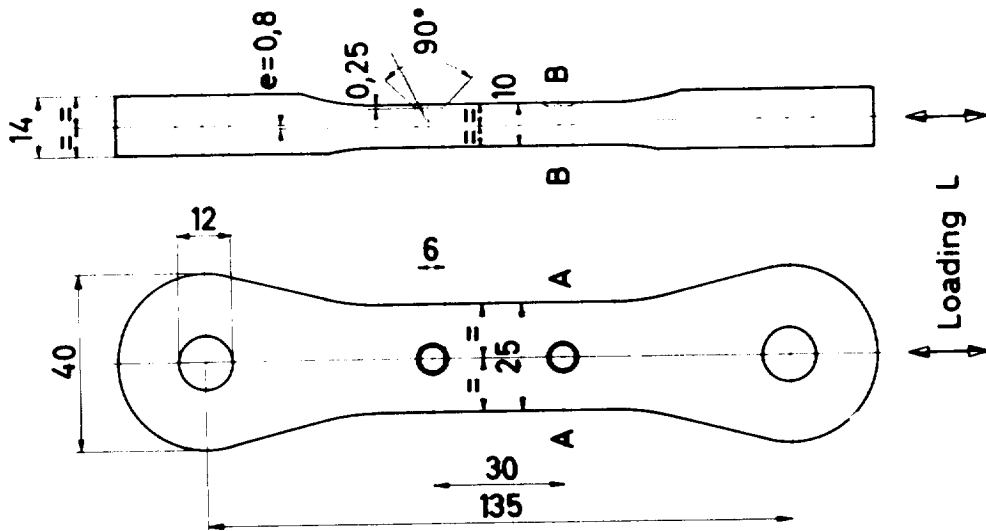
- For axial loads on 6 rods, tension and compression, up to 8 tons for each rod.
- Frequency 1 to 240 cpm
- Genuine sequence of loads
- 127 Load levels available
- Fully automatic electronic control, up to 120 000 orders in an unique and uninterrupted sequence .

Figure 2

"ICAF"-Test Rod for Light alloys

$$\sigma_n = \frac{L}{10(25-6)} = \frac{L}{190} \text{ kp/mm}^2$$

reamed after anodic surface treatment (if any was applied)

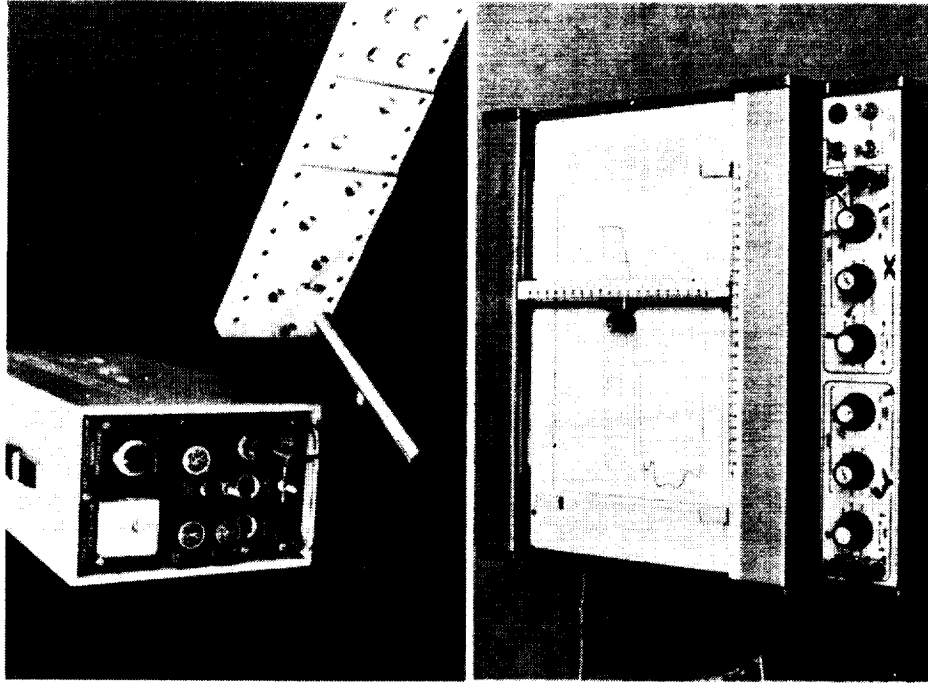


A-A

B-B

$K_1 = 3.24$
 $K_2 = 0.95$
 calculated by RAS Data Sheets
 $\frac{\sigma_b}{\sigma_n} = 0.48$, if elastic deformation by bending is neglected (universal suspension)

Figure 3



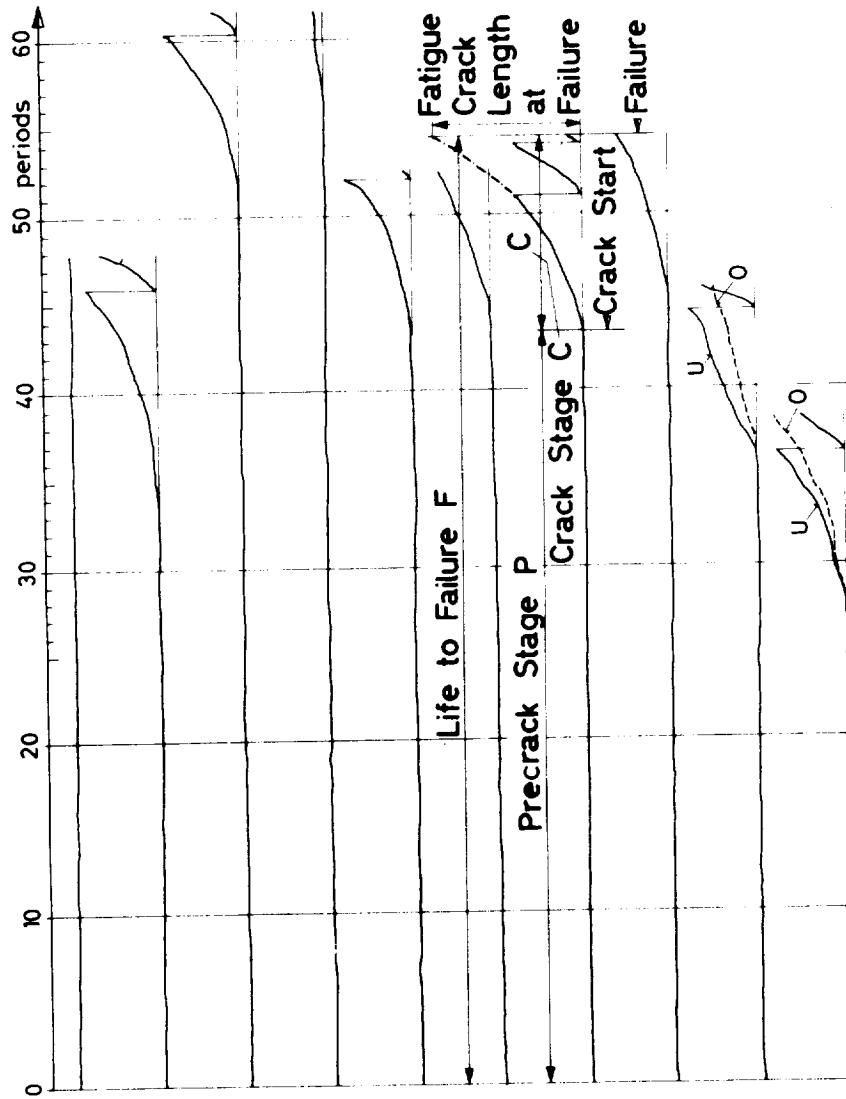
Eddycurrent

Crack Detector Type 02 (F+W)

- For non-ferromagnetic alloys
- For holes 4 to 50 mm diameter and flat surfaces
- 5 to 1 Volt output per 0.1 mm crack depth
- Range up to 50 Volts
- Indication independent of scratches or undulations up to 0.5 mm or of conical holes up to 5°

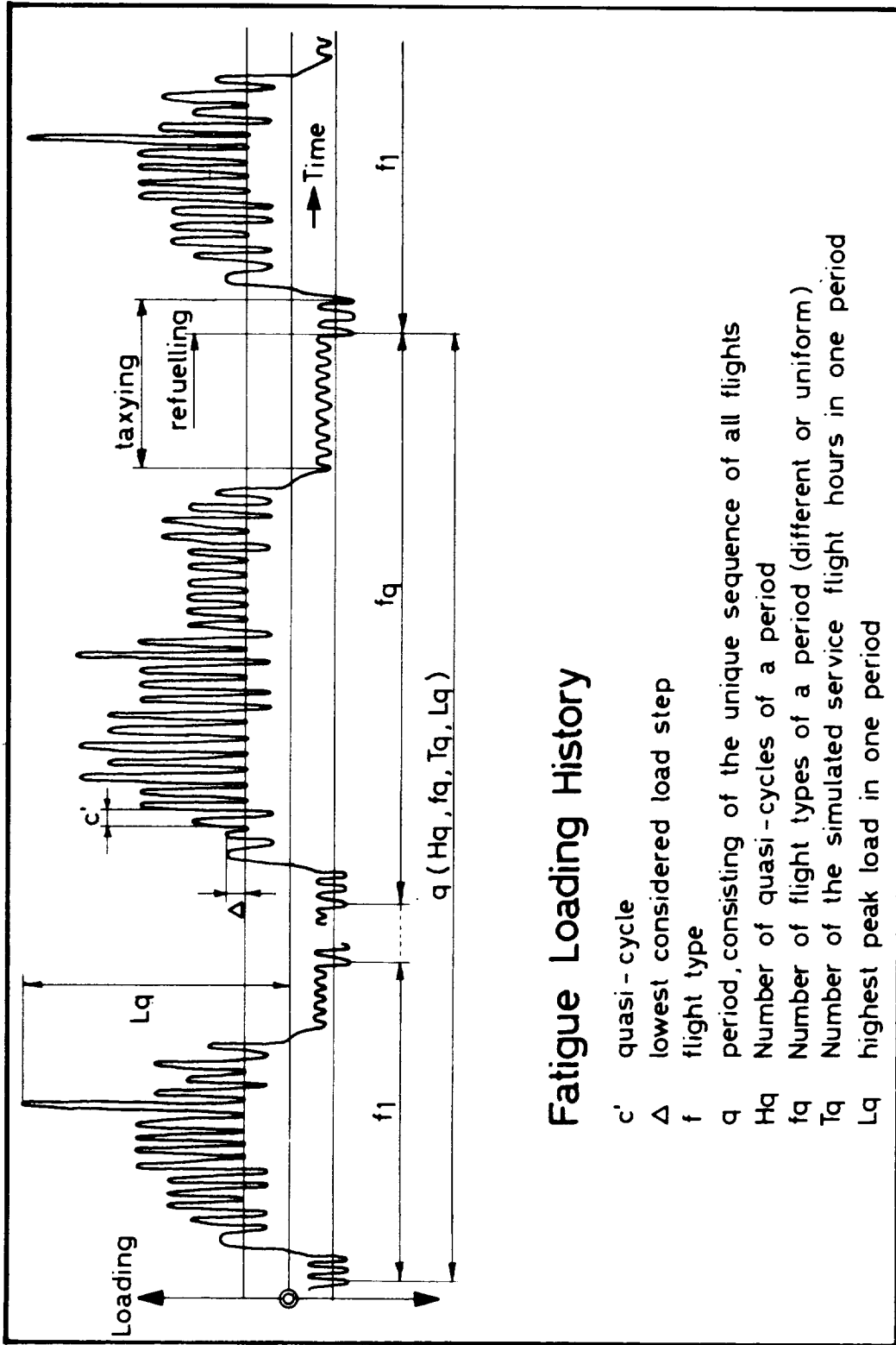
Figure 4

Crack Story of 12 Holes in 6 Rods automatically recorded by the Crack Detector Type 02



test run No.90 program XVIII/100/5265			
rod No. hole	crack start No. of periods	crack start No. of periods	failure No. of periods
E-144 o	—	—	—
E-144 u	34,4	47,821	—
E-143 o	51,4	61,406	—
E-143 u	56,4	—	—
E-142 o	43,4	52,406	—
E-142 u	44,4	—	—
E-141 o	43,4	54,406	—
E-141 u	45,8	—	—
E-140 o	37,4	45,839	—
E-140 u	36,4	—	—
E-139 o	27,4	—	—
E-139 u	27,4	38,406	—

Figure 5



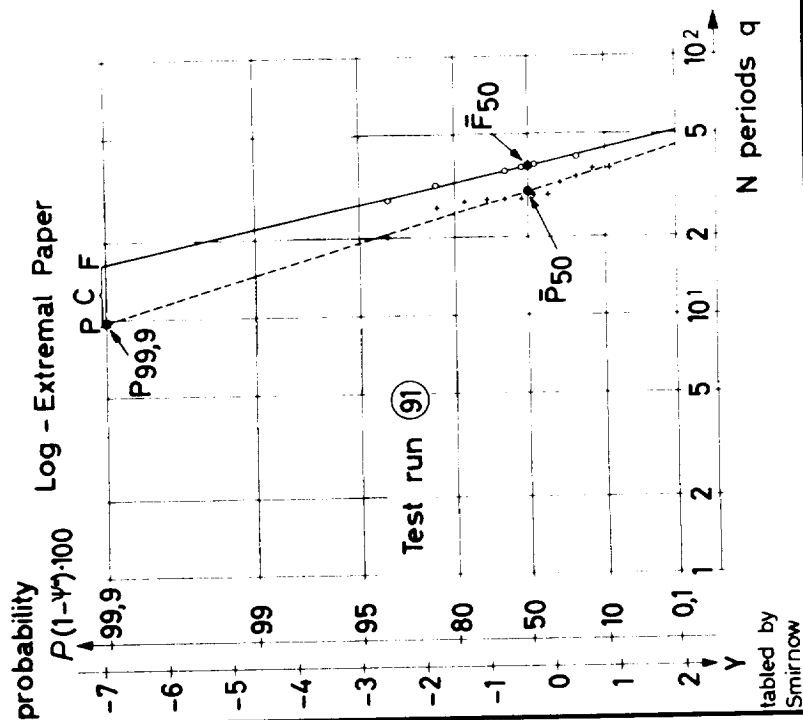
Fatigue Loading History

- c' quasi - cycle
- Δ lowest considered load step
- f flight type
- q period, consisting of the unique sequence of all flights
- Hq Number of quasi-cycles of a period
- fq Number of flight types of a period (different or uniform)
- Tq Number of the simulated service flight hours in one period
- Lq highest peak load in one period

Figure 6

Symbols s and \bar{N}

- n = number of holes (two per specimen)
- N = Number of periods q (350 flights per period)
- s = empirical standard deviation = $\left[\frac{1}{n-1} \sum_{i=1}^n (\log N_i - \log \bar{N}_b)^2 \right]^{1/2}$
- \bar{N}_a = arithmetical mean = $\frac{1}{n} \left(\sum_{i=1}^n N_i \right)$
- $\bar{N}_b = \sigma$ = probable mean = line of least squares at 50% probability of survival
- P = crack start (N)
- F = Failure (N)
- C = F - P = Crack stage
- \bar{P}_{50} = probable mean of crack start
- \bar{F}_{50} = probable mean of failure
- $\bar{C}_{50} = \bar{F}_{50} - \bar{P}_{50}$
- fs = scatter factor = $\frac{\bar{F}_{50}}{P_{99.9}}$



tabled by Smirnow

Figure 7

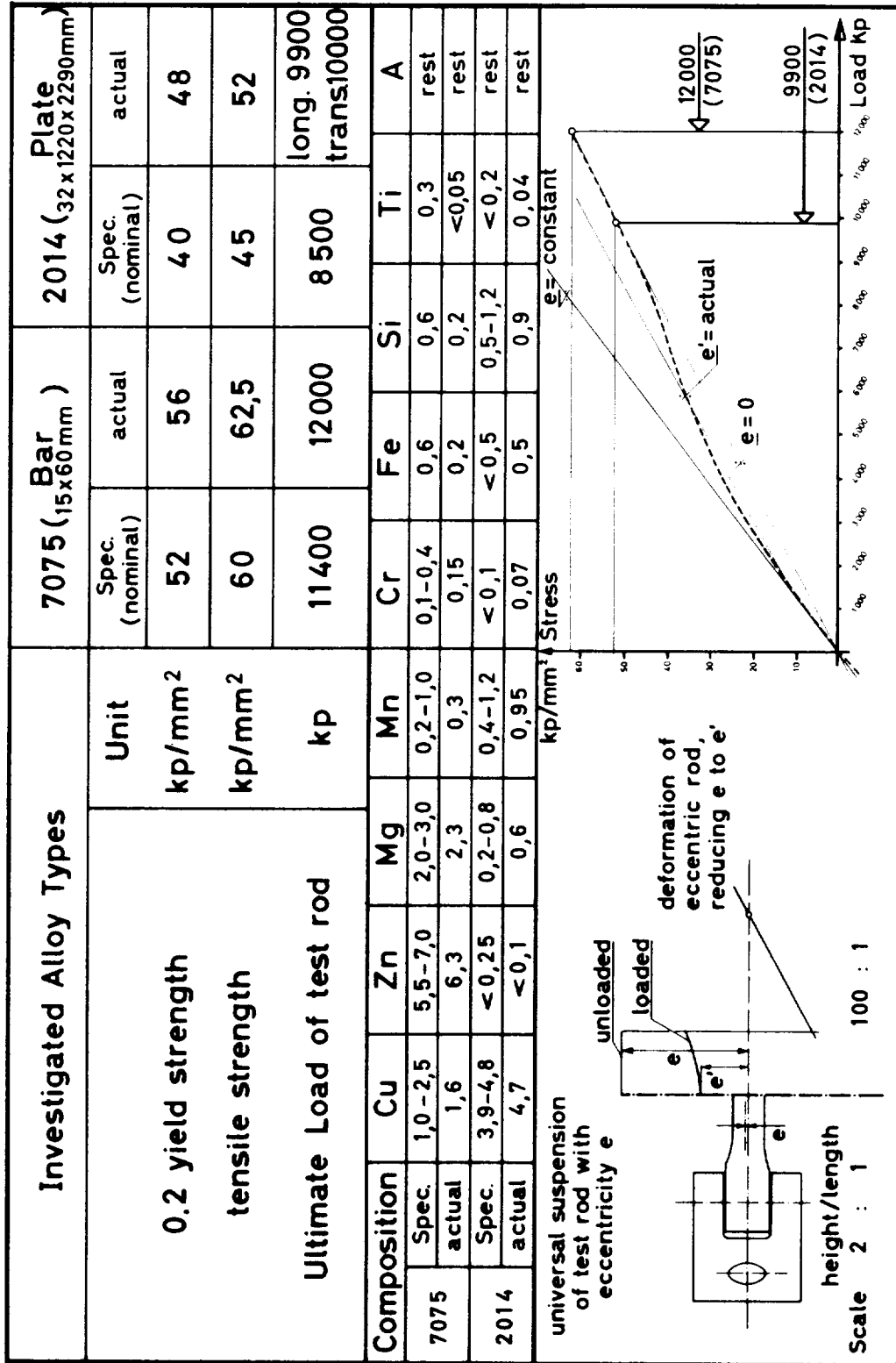


Figure 8

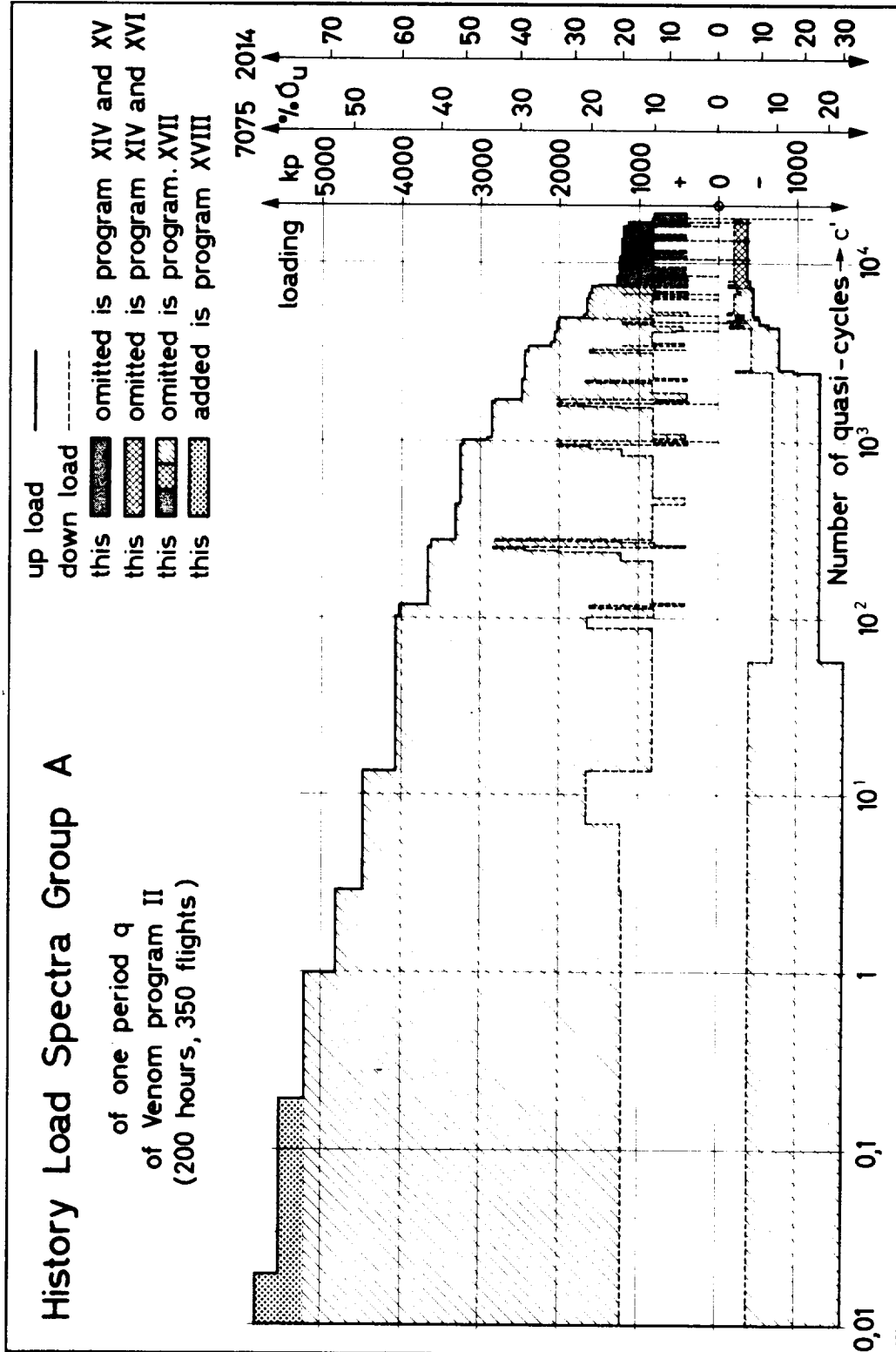


Figure 10

Program - Modification Group A

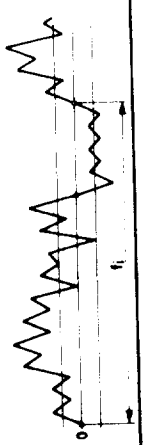
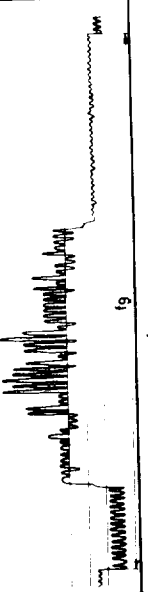
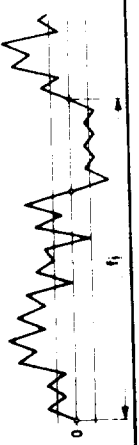
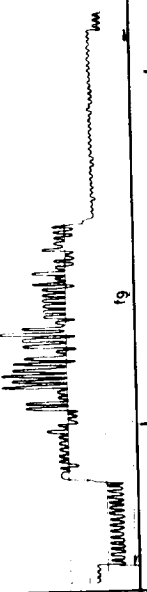
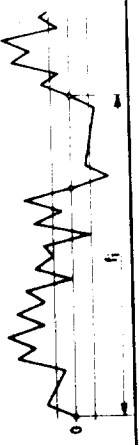
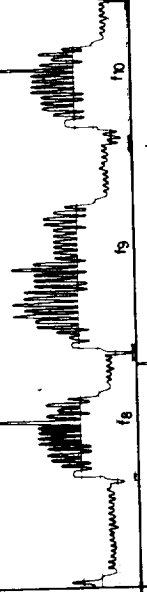
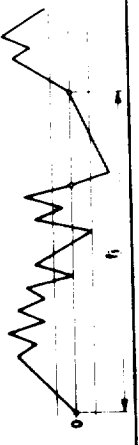
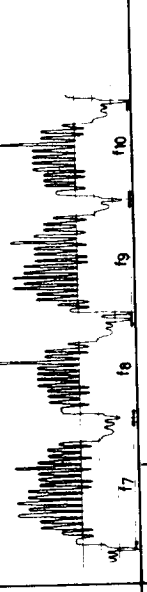
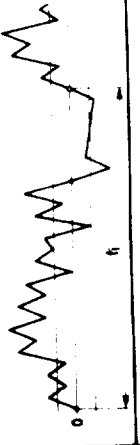

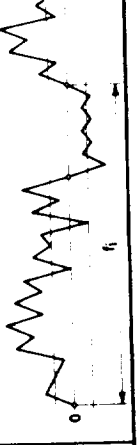
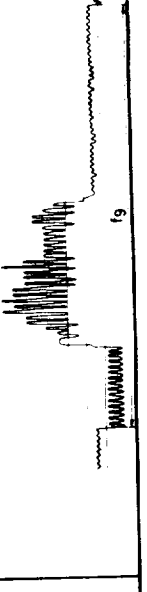
Program No.		No. of cycles per q in air	No. of cycles per q on ground	Schematic presentation	actual flight No. 9
XVIII	20033	18515			
II	20033	18515			
XIV	9180	3405			
XVII	6499	835			
XVI	20033	3405			
XV	9180	18515			

Figure 11

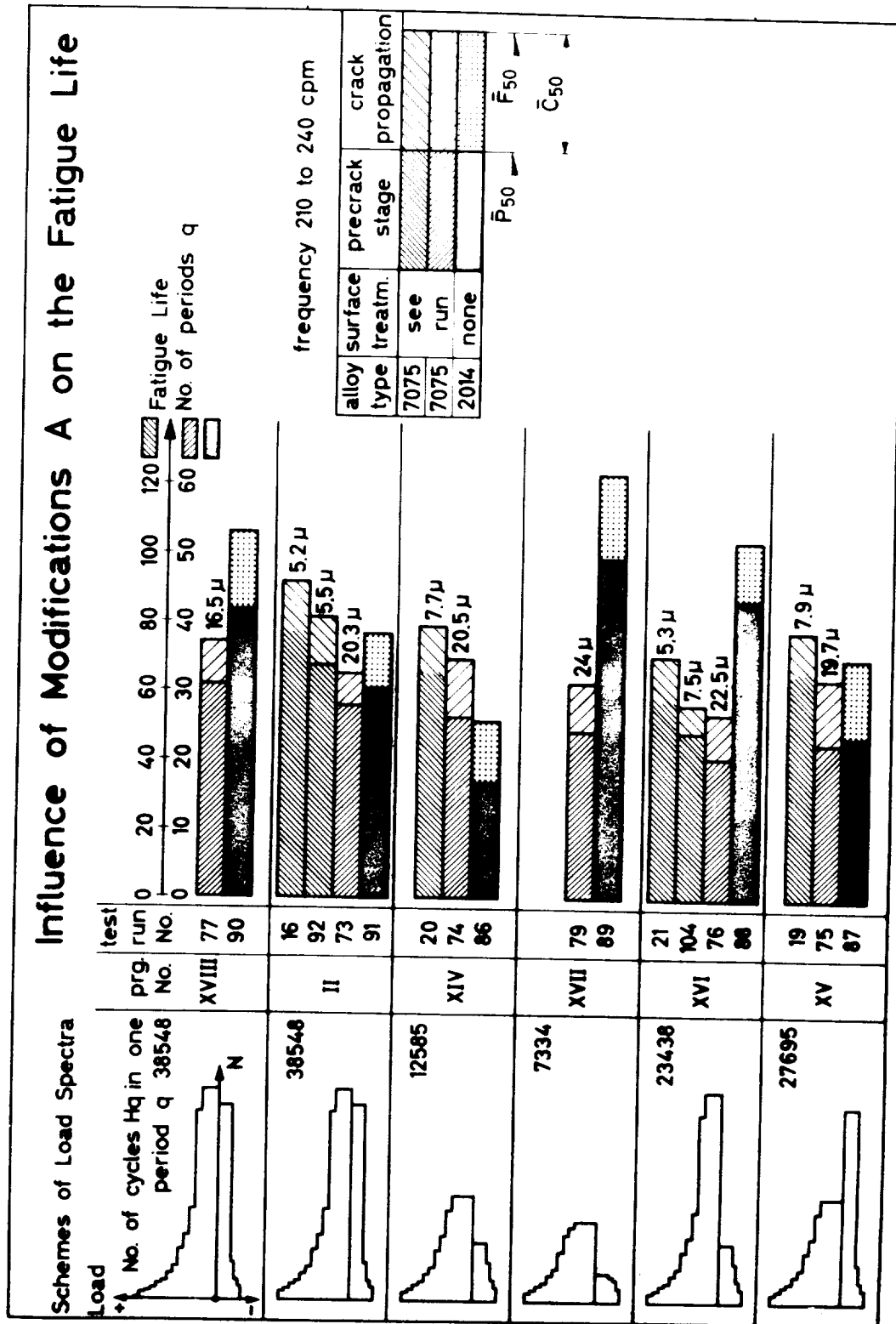


Figure 12

Load Spectra Group B

for one period q

- basic Venom program II
 - up load
 - down load
- this omitted is program V'
 - only peaks between +lg -crossings counted
- this omitted is program VI'
 - only peaks between zero-crossings counted
- derivations from Venom program II:
 - program XX: level crossing method
 - positive and negative peaks pooled
 - program XXI: range pair method
 - positive and negative peaks pooled
 - ground loads in program XX and XXI

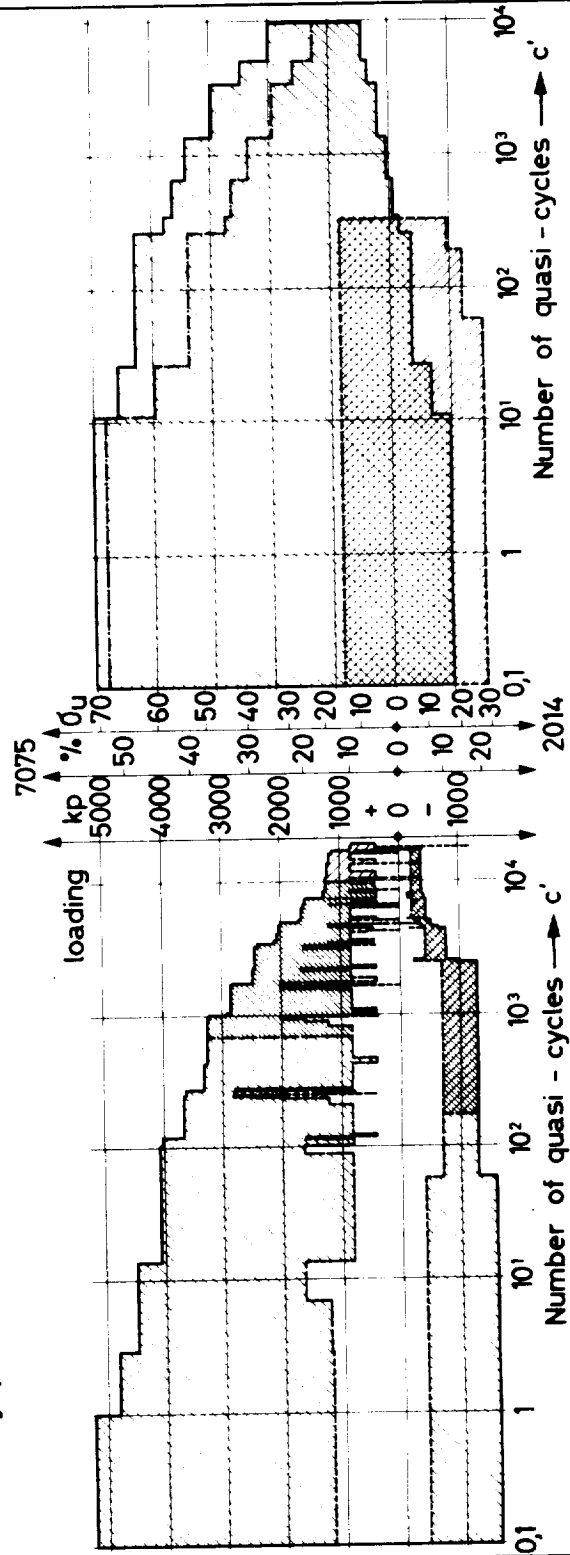


Figure 13

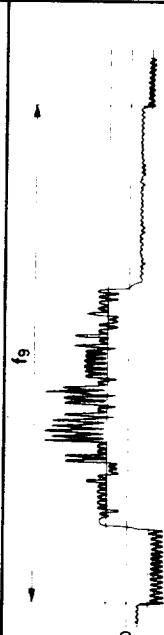
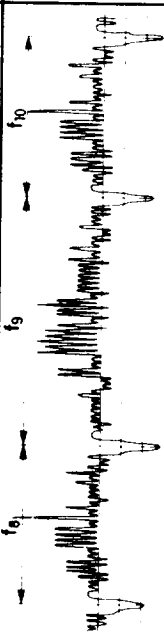
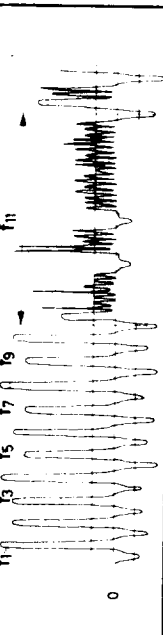
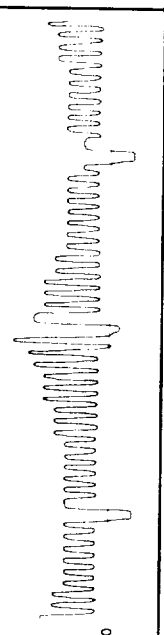
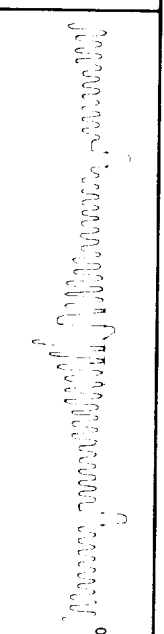
Program - Modification Group B			
Program No.	Actual program		No of cycles per q in air on ground
II		basic program reduced to the following count methods=	20033 18515
V'		mean - crossing peak, mean = +1g air	19553 350
VI'		mean - crossing peak, mean = 0g level	638 350
XX		level crossing (pooled blocks per flight)	10150
XXI		range pair (pooled blocks per flight)	10150

Figure 14

Influence of Modifications B on the Fatigue Life

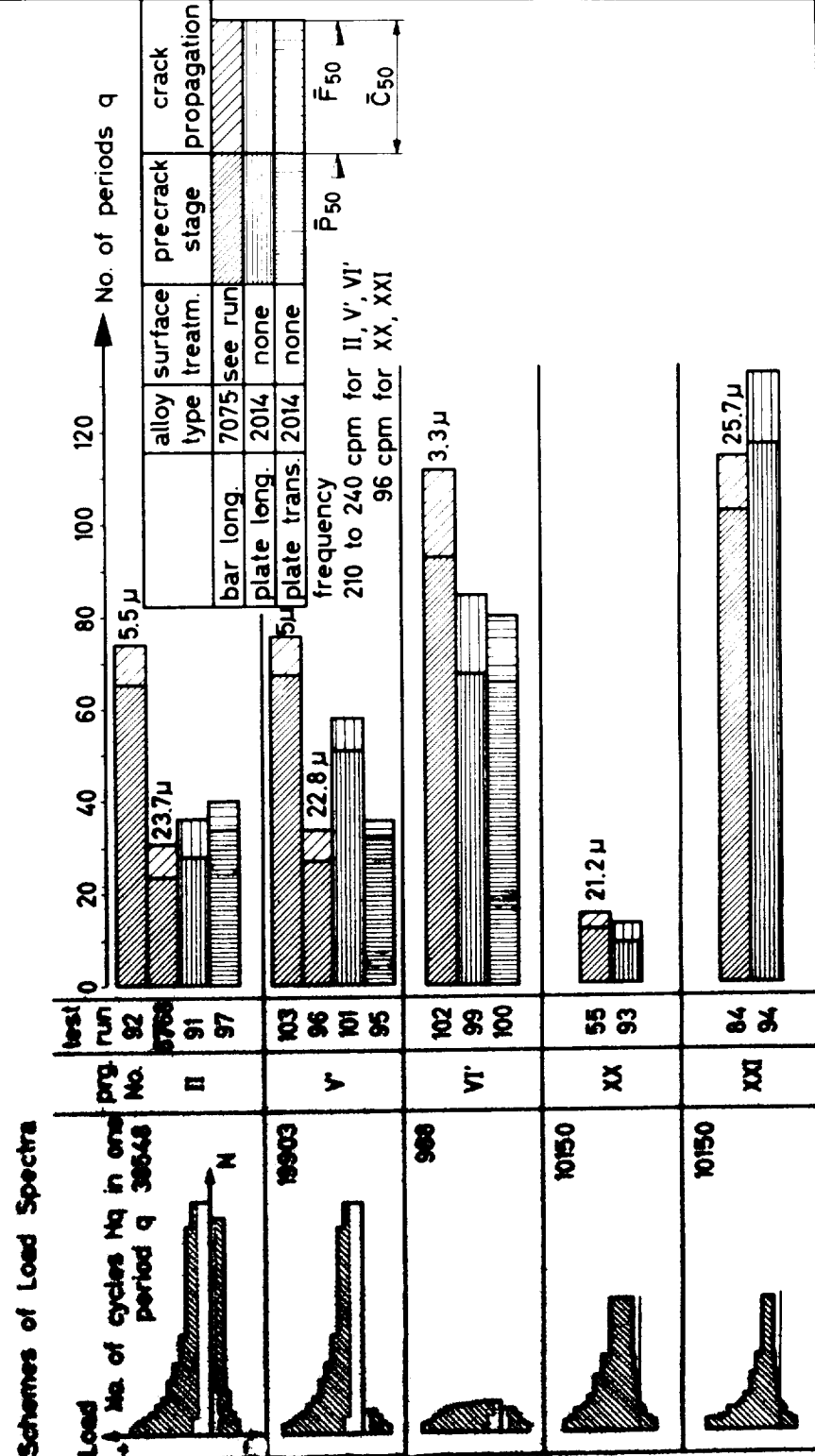


Figure 15

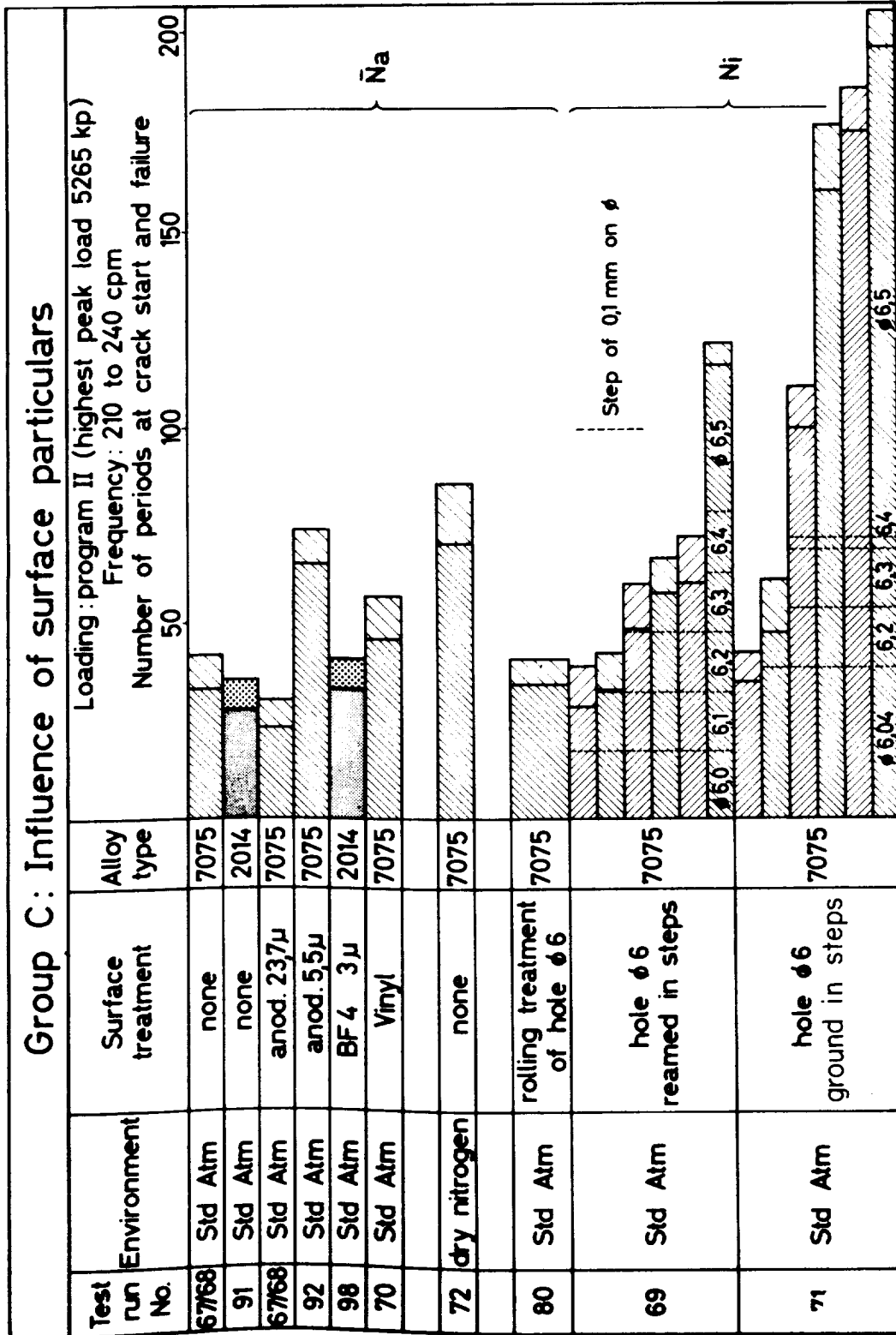


Figure 16

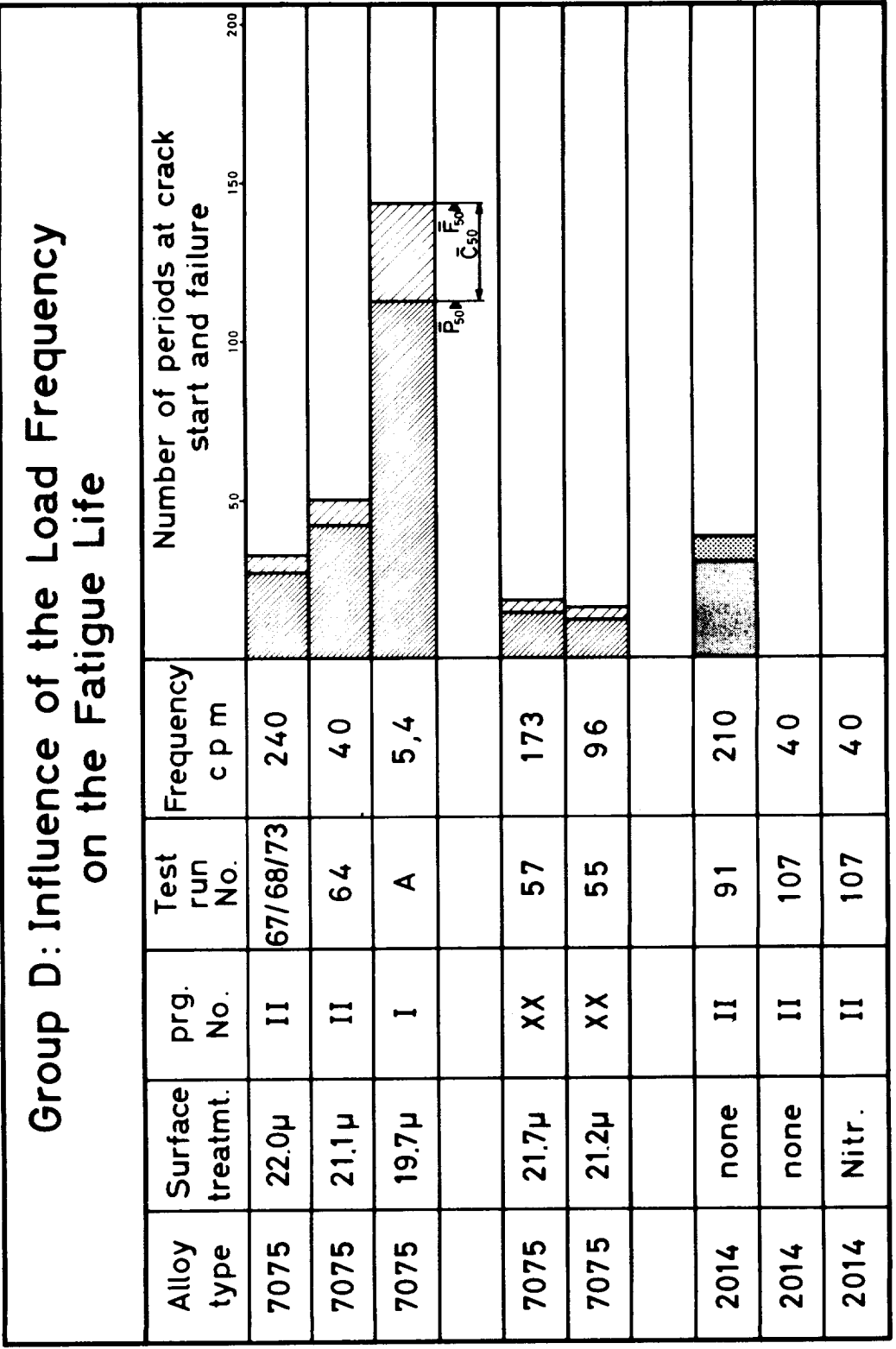


Figure 17

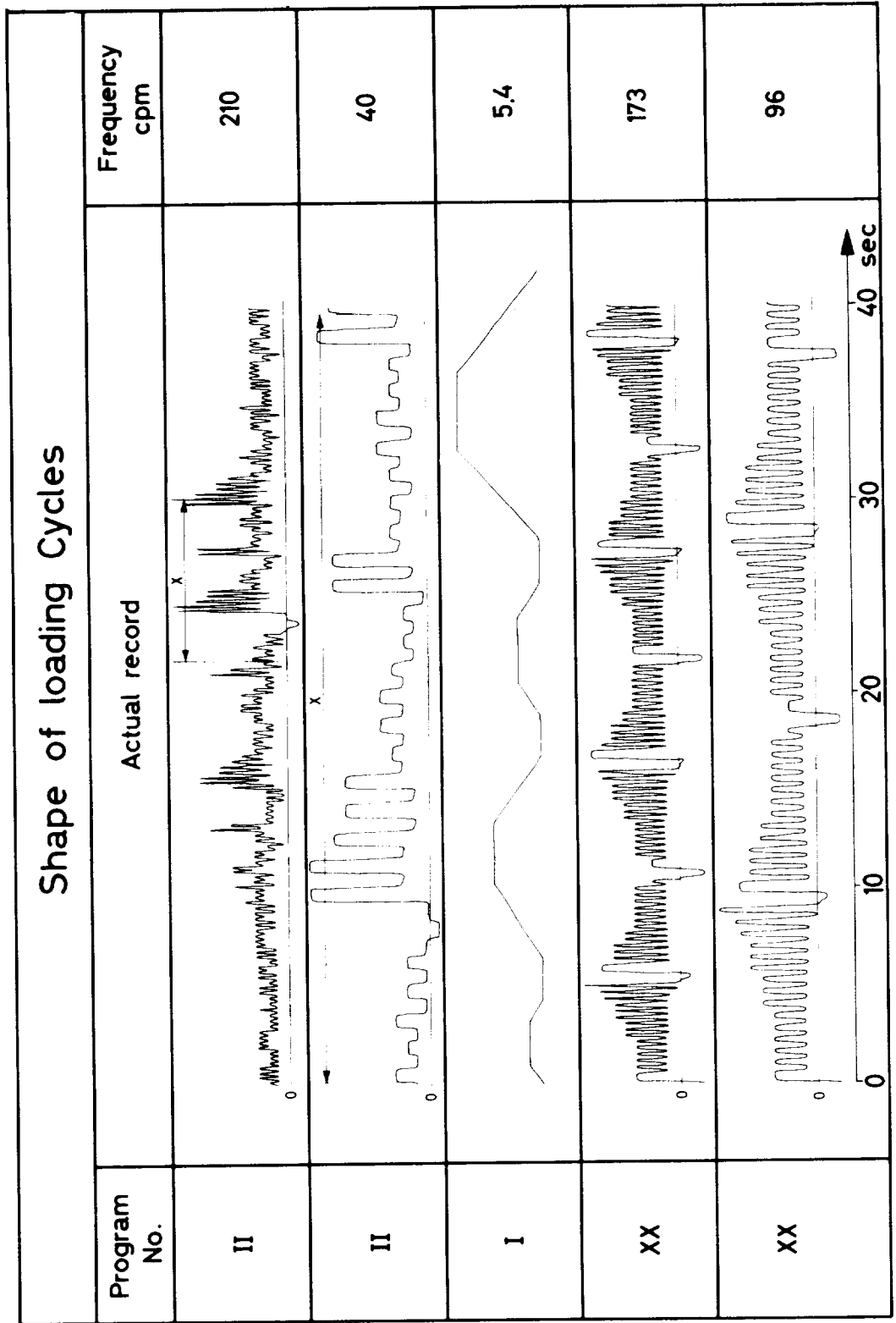


Figure 18

C.10

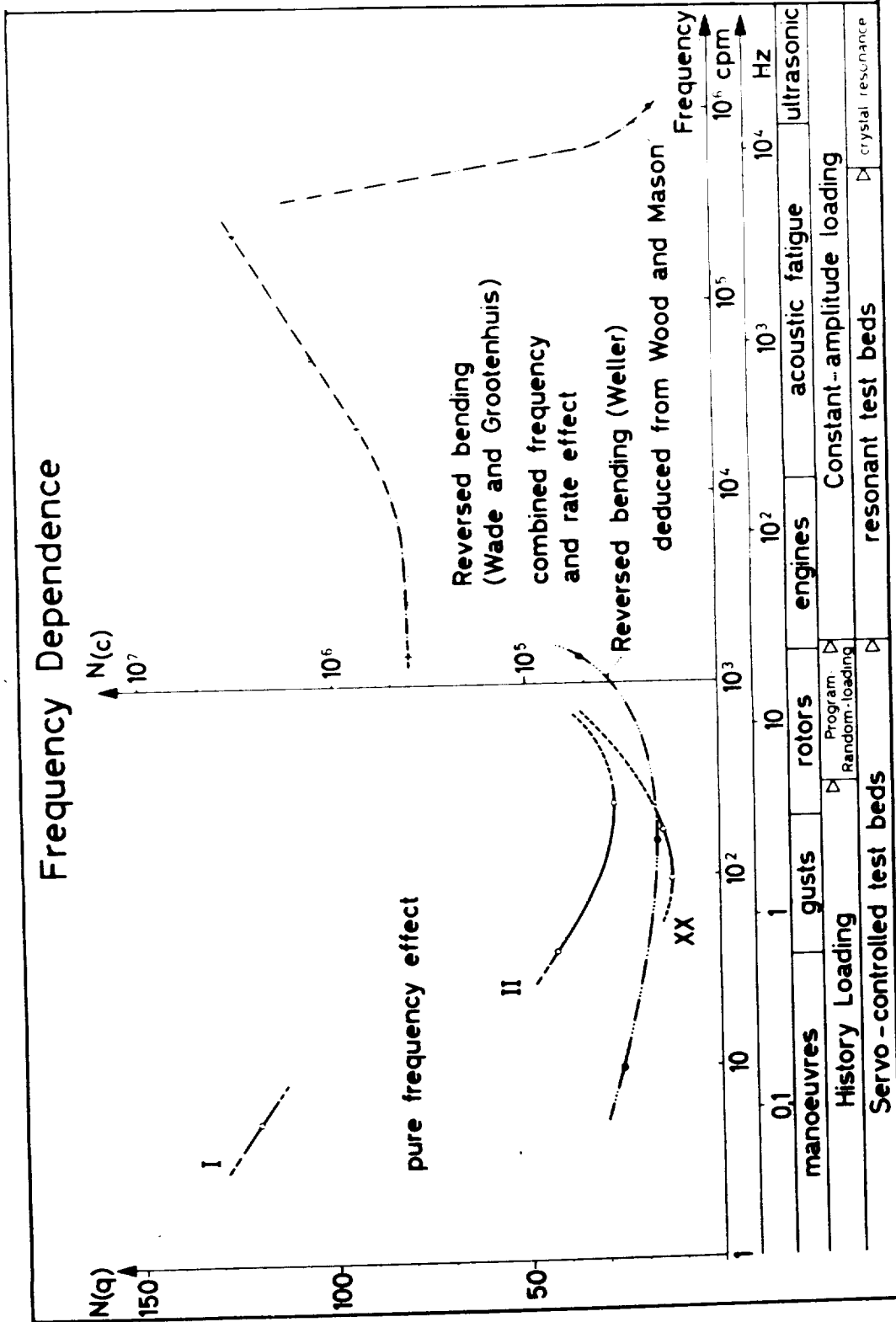


Figure 19

Scheme of the Influence of the chemical Activity

- S = Range of strain in one half-cycle
- v = Rate of straining = $\frac{dS}{dt}$
- I = Intensity of incitation of chemical activity = $f(v) \cdot f(S)$
- v = Rate of reaction = $f(I \cdot \frac{A}{\lambda})$
- A = chemical Affinity between the contacting mediums
- λ = chemical Resistance (e.g. oxide-layer) = $f(N, I, A)$
- p = Duration of reaction = persistence = $f(v)$
- R'' = amount of reaction in one half-cycle = $f(p, v, \omega)$
- D'' = Damage produced by R'' (e.g. oxide) = $f(R'')$
- ω = frequency of cycles
- R' = effective amount of reaction per cycle = $f(R'', \omega)$
- N = Number of cycles, periods
- D' = amount of damage produced in one cycle = $f(N, R')$

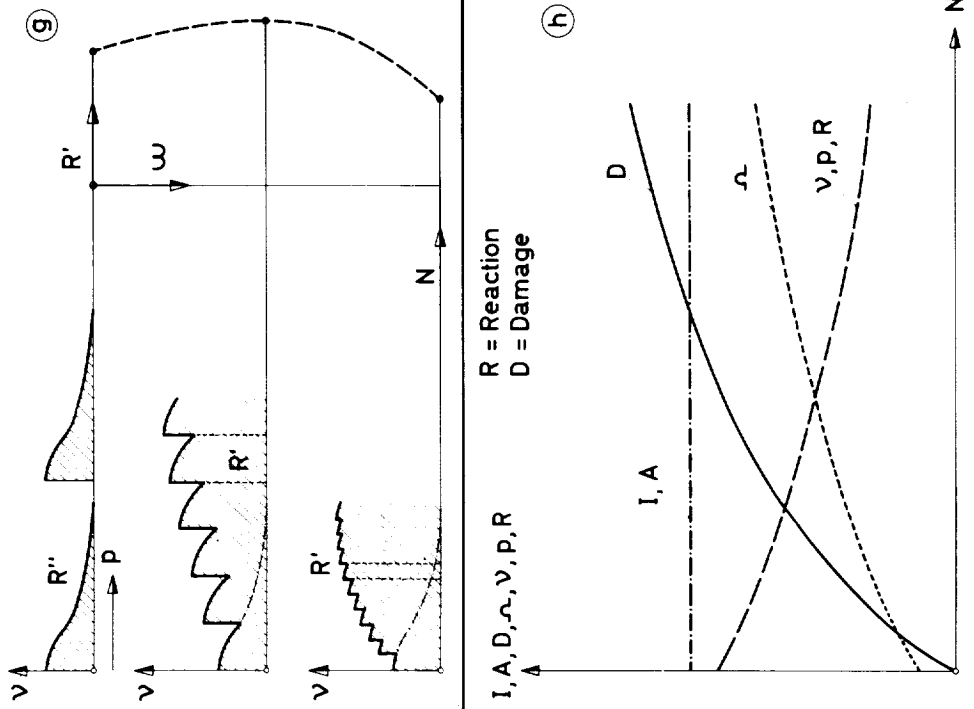


Figure 20

Scheme of the flake phase

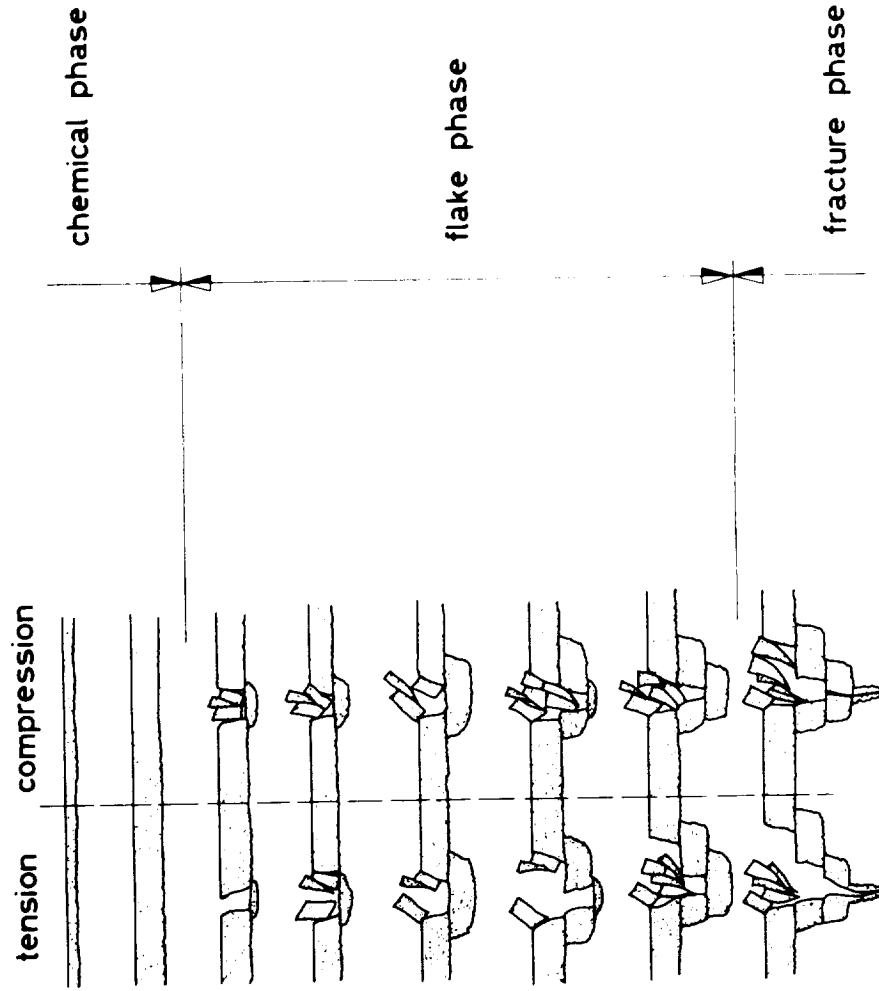


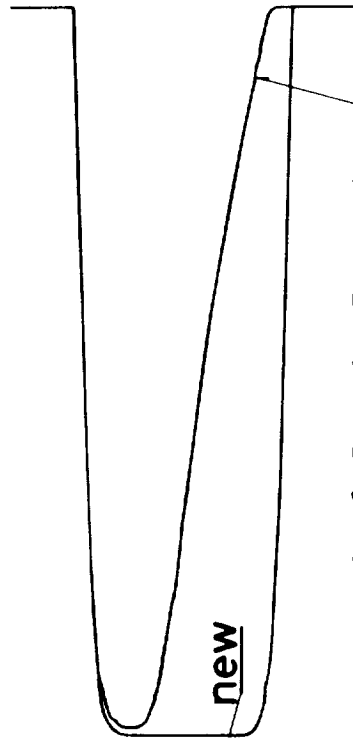
Figure 21

Fatigue Crack Surface

of test rod E102



Failure surface



Record of Crack Detector
before failure

Static failure Load : 9900 kp
new (mean value)
E 102 with fatigue crack 5890 kp

Figure 22

Probable Crack - Stage Life

as a function of the probability of survival

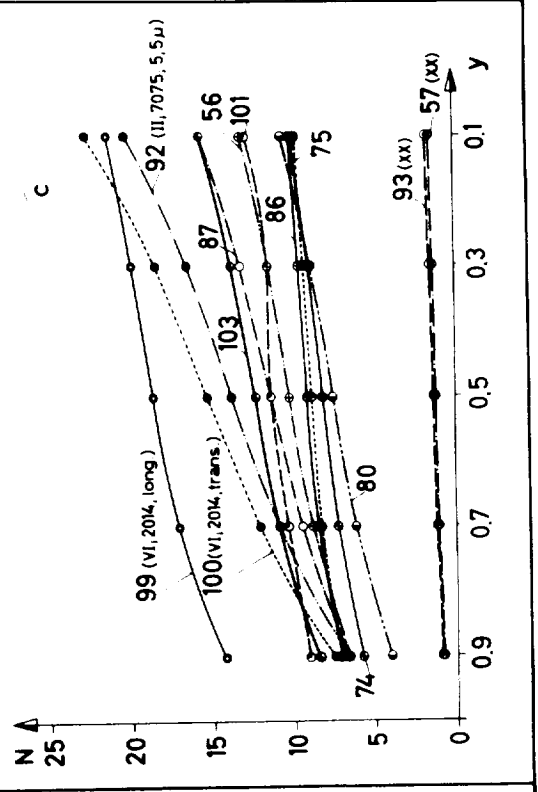
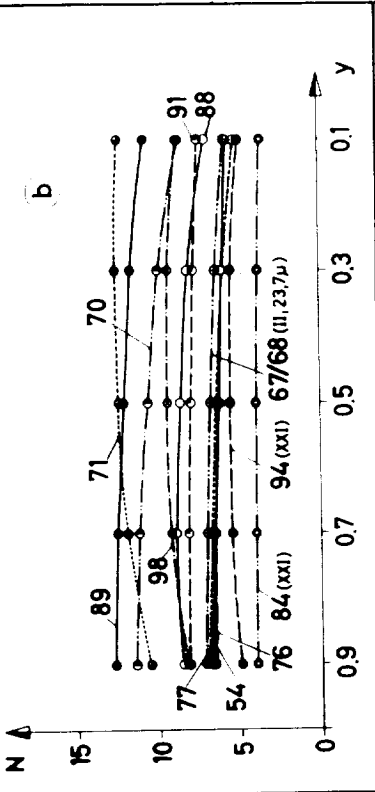
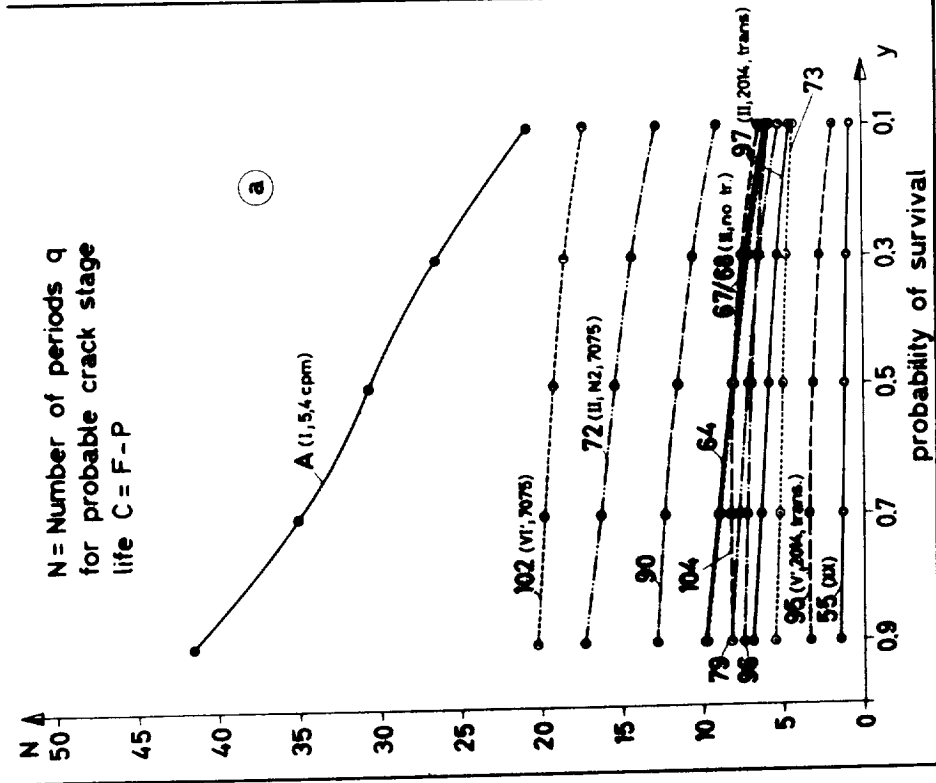


Figure 23

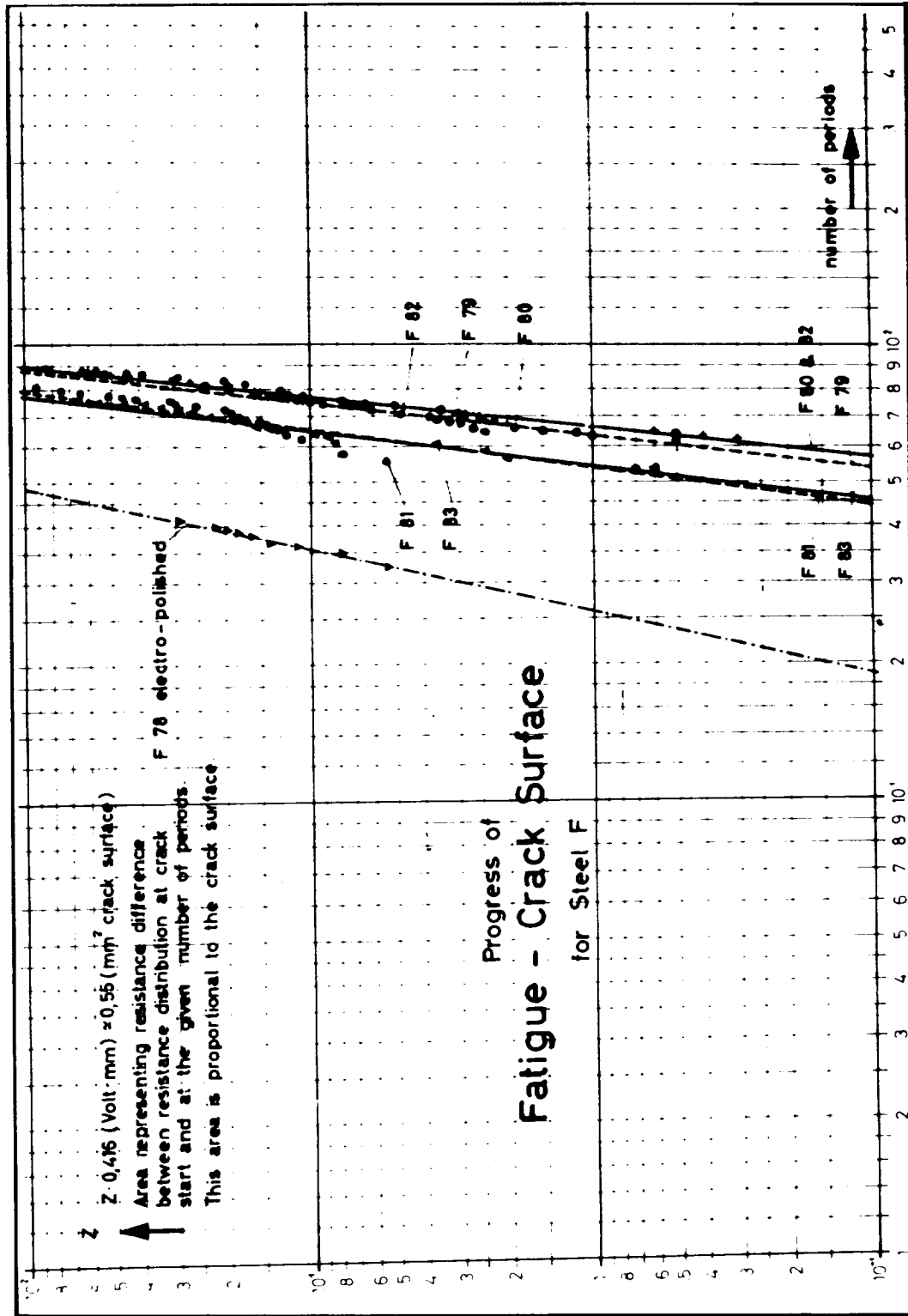


Figure 24

Scheme of the three damage phases

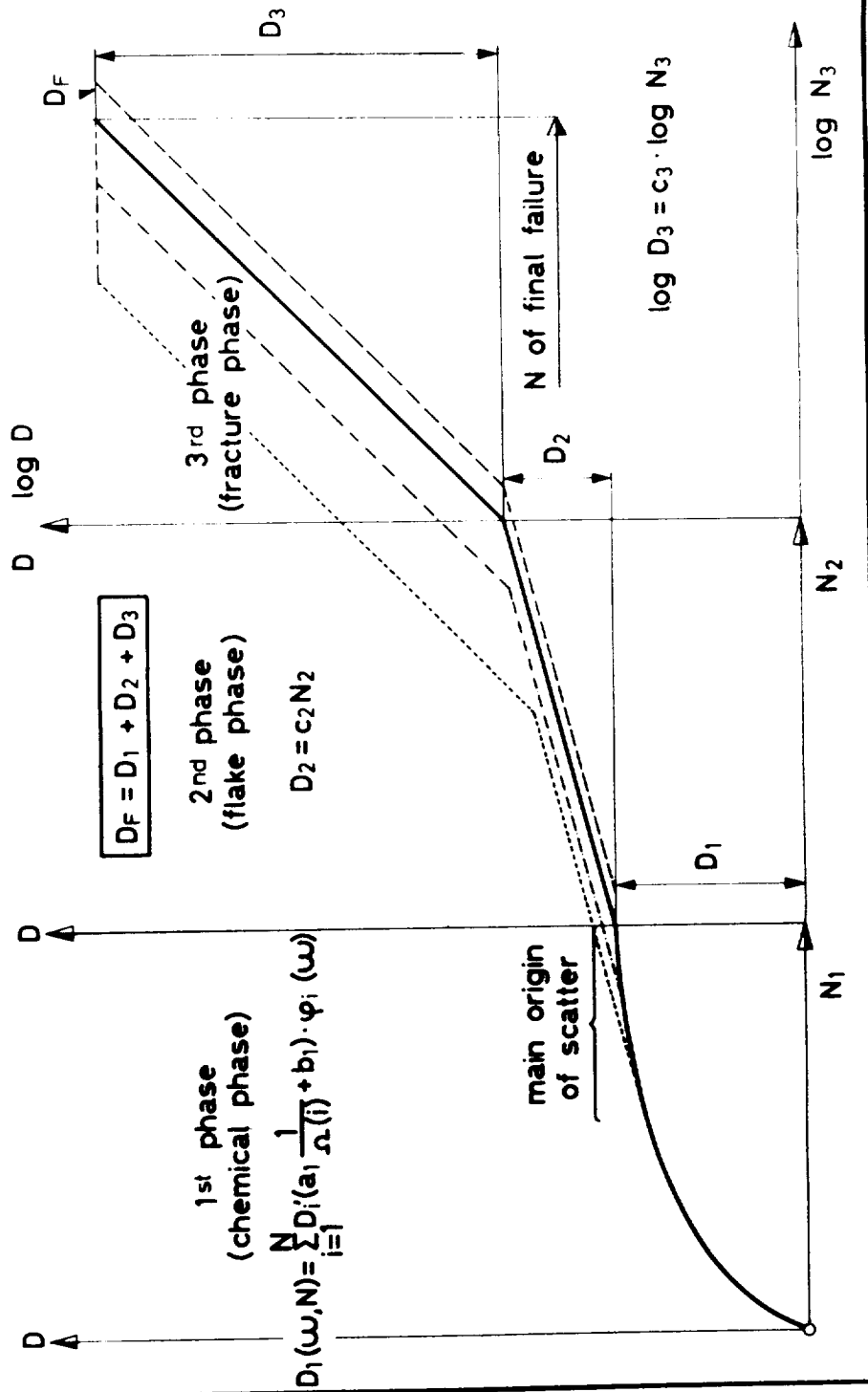


Figure 25

